

# **A Steady-State Pressure Model for Water Flow in a Hydraulically Fractured Geothermal Reservoir**

**Developed for further understanding of the  
potential of enhanced geothermal systems  
(EGS) in the Cooper Basin, South Australia**

**William Cibich**



**February  
2008**

## Abstract

The aim of this report was to develop a steady-state mathematical model that could describe water flow through an enhanced geothermal system (EGS) from injection wellhead to production wellhead. The model was to be implemented in Microsoft Excel® and put through sensitivity analyses to assist PIRSA in determining the potential and feasibility of geothermal energy in the Cooper Basin in South Australia. Well flow was modelled as flow through vertical pipes whilst fracture flow was modelled as flow between horizontal parallel plates and discs containing an element of roughness. The model was derived from traditional pipe flow equations and a combination of exact and approximate solutions to the Navier-Stokes equations. The model was implemented in Microsoft Excel® and sensitivity analyses were conducted to determine the effect of:

- mass flow rate
- fracture aperture
- fracture width
- number of fractures
- rock roughness and
- reservoir temperature

on injection pressure and production pressure, reservoir pressure profile, reservoir pressure drop and model validity. The results showed that for favourable reservoir geometries it is possible to operate EGS as a closed system with production pressure exceeding required injection pressure. This was attributed to less pressure drop occurring in the production well than in the injection well as a result of changes in water properties. The reservoir pressure profile analysis showed that the model was able to determine the pressure of flow along any point of the fractures. The largest pressure drop in the reservoir was found to occur during radial flow around the wellbore due to acceleration of the water. The most influential variable on reservoir pressure drop was found to be fracture aperture. This result emphasised the importance of hydraulic fracturing. Rock roughness was determined to cause deviation of the model from the cubic law. The model was valid for most reservoir geometries and only invalid for unfavourable scenarios. Recommendations were made that the model should be modified to include additional elements such as multiple fracture zones and fracture interconnectivity. A more precise solution to the radial Navier-Stokes problem should be found and turbulence around the wellbore should be investigated further. The model should be extended to include the electricity production process so that the potential of EGS can be better understood. The long-term goal for the model is to convert it from steady-state to transient in order to determine reservoir lifetime and understand the position of EGS in South Australia in the future.

## Contents

Introduction .....	1
Project Statement .....	1
Model Description.....	1
Flow Geometry.....	1
Well Flow Modelling .....	3
Fracture Flow Modelling.....	4
Water Properties.....	7
Model Limitations .....	7
Excel Program.....	8
Sensitivity Analysis.....	11
Mass Flow Rate Analysis.....	11
Fracture Aperture Analysis .....	11
Fracture Width Analysis .....	11
Number of Fractures Analysis .....	11
Roughness Analysis .....	12
Reservoir Temperature Analysis.....	12
Results .....	13
Mass Flow Rate.....	13
Fracture Aperture .....	14
Fracture Width .....	16
Number of Fractures .....	18
Roughness .....	20
Reservoir Temperature.....	21
Discussion .....	23
Required injection pressure and resulting production pressure .....	23
Reservoir Pressure Profile.....	24
Reservoir Pressure Drop .....	24
Model Validity .....	26
Recommendations .....	27
Conclusions.....	28
Nomenclature .....	29
Conversion Factors.....	30
References.....	31
Appendix A: Model Derivation .....	32
Linear Flow .....	32
Radial Flow .....	36
Overall Reynolds Number.....	42
Assumption Validation.....	43
Appendix B: Sample Calculation.....	45
Appendix C: Sensitivity Analysis Data.....	53

# Introduction

## Project Statement

The purpose of this project was to:

- Develop a mathematical steady-state pressure model for water flow in a hydraulically fractured geothermal reservoir in order to assist PIRSA in determining the potential and feasibility of enhanced or engineered geothermal systems (EGS) in the Cooper Basin, South Australia.
- The model was implemented in Microsoft Excel® and put through sensitivity analyses to determine the effect of:
  - o mass flow rate
  - o fracture aperture
  - o fracture width
  - o number of fractures
  - o rock roughness and
  - o reservoir temperatureon injection pressure and production pressure, reservoir pressure profile, reservoir pressure drop and model validity.

## Model Description

### Flow Geometry

The geometry of the model, shown below in figure 1, is designed to resemble an EGS with a reservoir created by hydraulic stimulation procedures. The model consists of three sections: injection well, fractured reservoir and production well. Barefoot completion is assumed for the wells. The reservoir is of length  $L$ , at a depth  $D$  and consists of  $n$  purely horizontal fractures. The fractures are assumed horizontal as overthrust stress conditions in the Cooper Basin produce predominately horizontal fractures when granite is hydraulic stimulated (Wyborn, de Graaf, Davidson & Hann 2004).

Flow within the model is as follows. Water at temperature  $T_i$  is injected down the injection well at wellhead pressure  $P_i$ . When the water reaches the reservoir it flows into the fractures. Each fracture is identical and consists of three flow regimes in series. First the water flows outwardly in a purely radial fashion from the injection wellbore at some angle  $\theta$  until it reaches the external radius,  $r_e$  (figure 2 (a)). At this point flow becomes linear along the fracture until it reaches the external radius of the production end and flows inwardly in a purely radial fashion towards the production wellbore (figure 2 (b)). The water then flows up the production well (at temperature  $T_p$ ) to reach the production wellhead at pressure  $P_p$ .

The angle of radial flow is determined by the orientation of the no-flow boundaries defined by the geometry of the fracture (Slider 1983). For example, if the fracture defines half a circle as the flow geometry, then  $\theta$  will be  $180^\circ$  as shown in figure 2. The method of combining three flow regimes in series is adopted from Slider (1983).

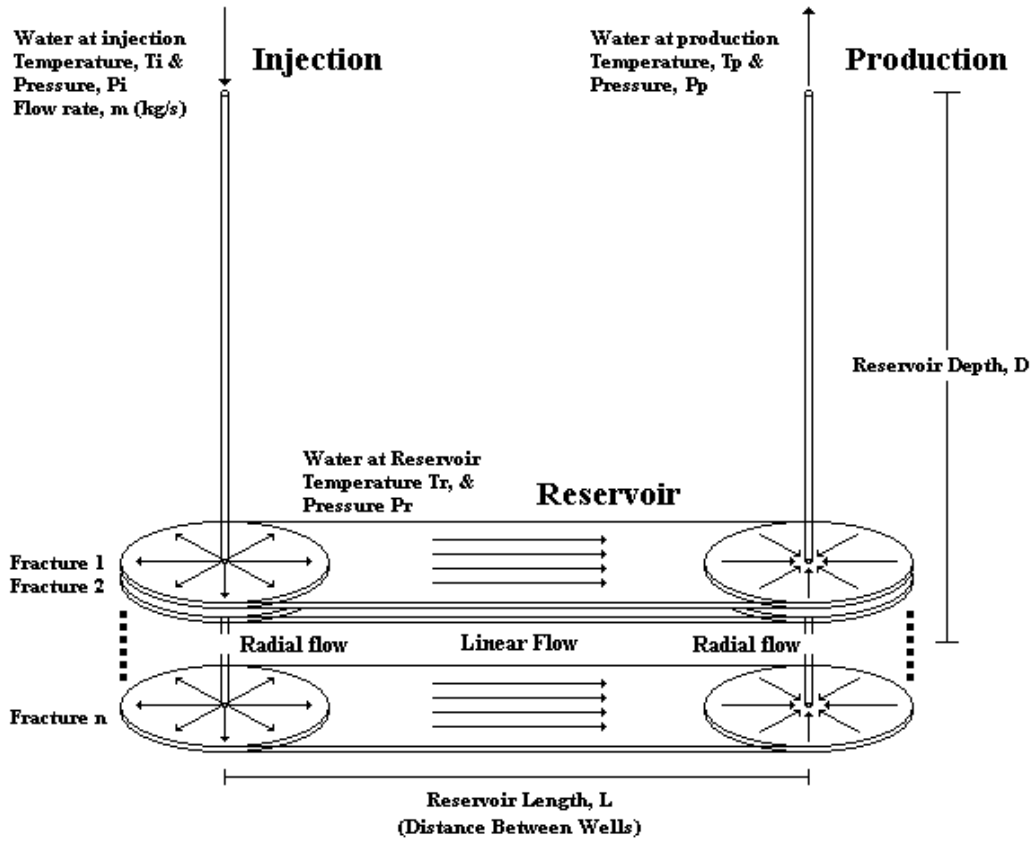


Figure 1 Geometry of the EGS model.

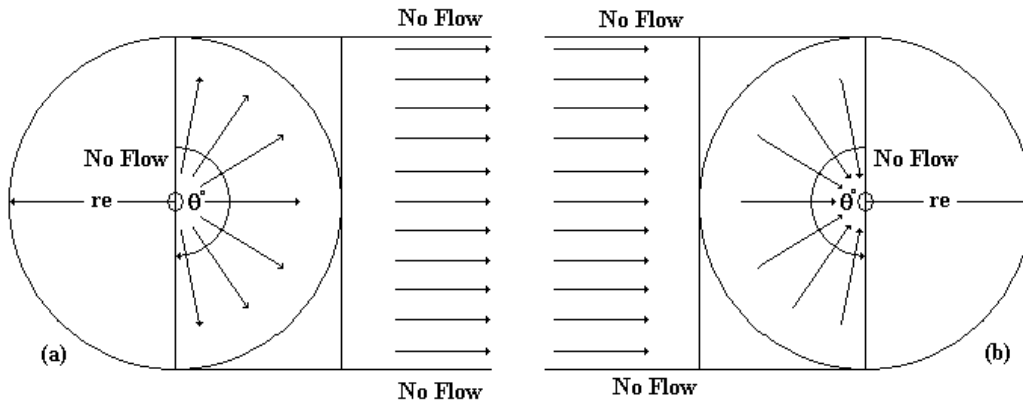


Figure 2 Plan view of a fracture displaying the three flow regimes in series, injection side (a), production side (b).

## Well Flow Modelling<sup>1</sup>

The injection and production wells are assumed completely vertical, constant in diameter and cased with commercial steel. Flow in the wells is modelled as traditional pipe flow. The flow is assumed fully developed. Equation 1 is used to determine pressure drop in the wells:

$$\Delta P_{i,p} = \rho g h_L - \rho g (z_1 - z_2) \quad (1)$$

where  $\rho$  is water density ( $\text{kg/m}^3$ ),  $g$  is gravitational acceleration ( $9.81 \text{ m/s}^2$ ),  $z$  represents vertical displacement at points 1 and 2 and  $h_L$  is the 'energy loss' determined by the Darcy-Weisbach equation:

$$h_L = f \left( \frac{D}{d_w} \right) \frac{\hat{u}^2}{2g} \quad (2)$$

where  $f$  is the friction factor,  $D$  is the depth of the well (hence the length of the casing) (m),  $d_w$  is the well diameter (m) and  $\hat{u}$  is the average velocity of the fluid (m/s). For turbulent flow the friction factor  $f$  is determined by the Colebrook equation:

$$f_1 = \frac{0.25}{\left\{ \log \left[ \frac{\varepsilon / d_w}{3.7} + \frac{2.51}{\text{Re} \sqrt{f_0}} \right] \right\}^2} \quad (3)$$

where the Reynolds number is ( $\mu$  is fluid dynamic viscosity ( $\text{kg/m.s}$ )):

$$\text{Re} = \frac{\rho \hat{u} d_w}{\mu} \quad (4)$$

and  $\frac{\varepsilon}{d_w}$  is the well relative roughness determined by Moody's Chart for commercial pipes.

Equation 3 requires an iterative approach where an initial guess value for friction is given by the Blasius equation:

$$f_0 = 0.3164 \text{Re}^{-1/4} \quad (5)$$

This initial guess is substituted into the Colebrook equation to yield a new value for  $f$ . The new  $f$  is substituted back into equation 3 and another new value for  $f$  is determined. This process is repeated until  $f$  converges to a certain tolerance level. Turbulence is assumed for  $\text{Re} > 2300$ . If  $\text{Re} \leq 2300$  the Darcy friction factor for laminar flow is:

$$f = \frac{64}{\text{Re}} \quad (6)$$

---

<sup>1</sup> The author acknowledges Munson, Young & Okiishi (2006) as the primary reference in this section.

## Fracture Flow Modelling<sup>2</sup>

Each fracture is assumed to be identical and therefore the total flow injected is modelled to divide evenly between  $n$  fractures. Thus the volumetric flow rate per fracture,  $q_{pf}$ , is equal to:

$$q_{pf} = \frac{m}{\rho n} \quad (7)$$

where  $m$  is the total mass flow rate (kg/s). The rock is assumed to be nonporous and thus flow through fractures is modelled as flow through horizontal parallel plates (in the case of linear flow) and discs (in the case of radial flow), of aperture  $h$ , containing an element of roughness,  $\varepsilon$ , as show in figure 3:

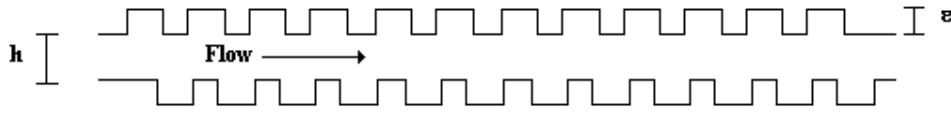


**Figure 3** Side view of a fracture with roughness element.

The boundaries of linear and radial flow are defined by parameters  $L$  (distance between wells),  $\theta$  (angle of radial flow) and  $w$  (fracture width), which are displayed in figure 4.

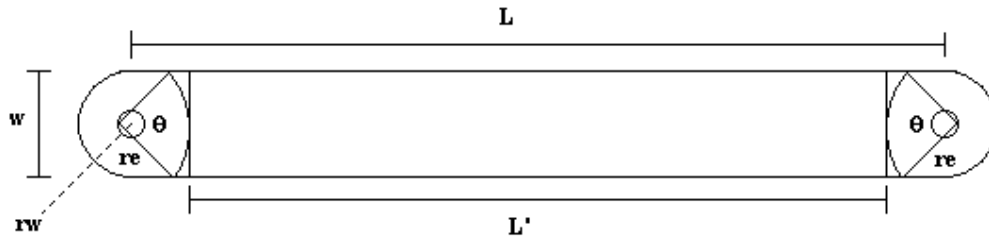


**Figure 4** Plan view of a fracture showing parameters defining boundaries of radial and linear flow.

The well radius,  $r_w$  is fixed but the external radius,  $r_e$  is dependent on  $\theta$  and  $w$  such that:

$$r_e = \frac{w}{2 \sin\left(\frac{\theta}{2}\right)} \quad (8a)$$

If  $\theta$  is equal to  $360^\circ$  then the equation for  $r_e$  is:

$$r_e = \frac{w}{2} \quad (8b)$$

<sup>2</sup> The derivation of this model is demonstrated in appendix A.

Thus the length of the linear section ( $L'$ ) is equal to:

$$L' = L - 2r_e \quad (9)$$

Thus it is possible that for a wide enough fracture no linear flow will exist and  $r_e$  is therefore limited to  $L/2$ . The expression for pressure drop in the linear section of flow is determined by equation 10:

$$\Delta P_{lin} = f_f \rho \frac{L'}{h} \hat{u}^2 \quad (10)$$

The expression for pressure drop in the radial section of flow is determined by equation 11:

$$\Delta P_{rad} = f_f \rho \frac{r_e - r_w}{h} \hat{u}_{rad}^2 \quad (11)$$

Where the average velocity  $\hat{u}$  in the radial section is defined by:

$$\hat{u}_{rad} = \frac{180q \ln\left(\frac{r_e}{r_w}\right)}{(r_e - r_w)\theta\pi h} \quad (12)$$

The Reynolds number for a fracture,  $Re_f$ , is calculated in the same manner as Jones, Wooten and Kaluza (1988) and Murphy, Coxon and McEligot (1978) in their studies of fluid flow between parallel plates and discs:

$$Re_f = \frac{2h\hat{u}\rho}{\mu} \quad (13)$$

The friction factor for fracture flow is adopted and modified from the experimental study by Louis (1969) and was expressed as:

$$f_f = \left( \frac{24}{Re_f} \right) \left( 1 + 3.1 \left( \frac{\varepsilon}{h} \right)^{1.5} \right) \quad (14)$$

This friction factor incorporates the relative roughness of the rock ( $\varepsilon/h$ ) and is applicable to a laminar flow regime. The total reservoir pressure drop is the sum of two identical radial sections and one linear section and is therefore given by:

$$\Delta P_r = \Delta P_{lin} + 2\Delta P_{rad} \quad (15)$$

It is assumed for the purposes of the model that in order to flow water into the reservoir, the injection wellbore pressure must be equal to the reservoir pressure plus half of the reservoir pressure drop. This would mean that the pressure of flow at the midpoint between wells should be equal to reservoir pressure,  $P_r$ . Therefore, in order for flow to reach the production wellbore, the

production wellbore pressure should be equal to the reservoir pressure minus half the reservoir pressure drop. This assumption is described mathematically and pictorially below:

$$P_{iw} = P_r + \frac{\Delta P_r}{2} \text{ and } P_{pw} = P_r - \frac{\Delta P_r}{2}$$

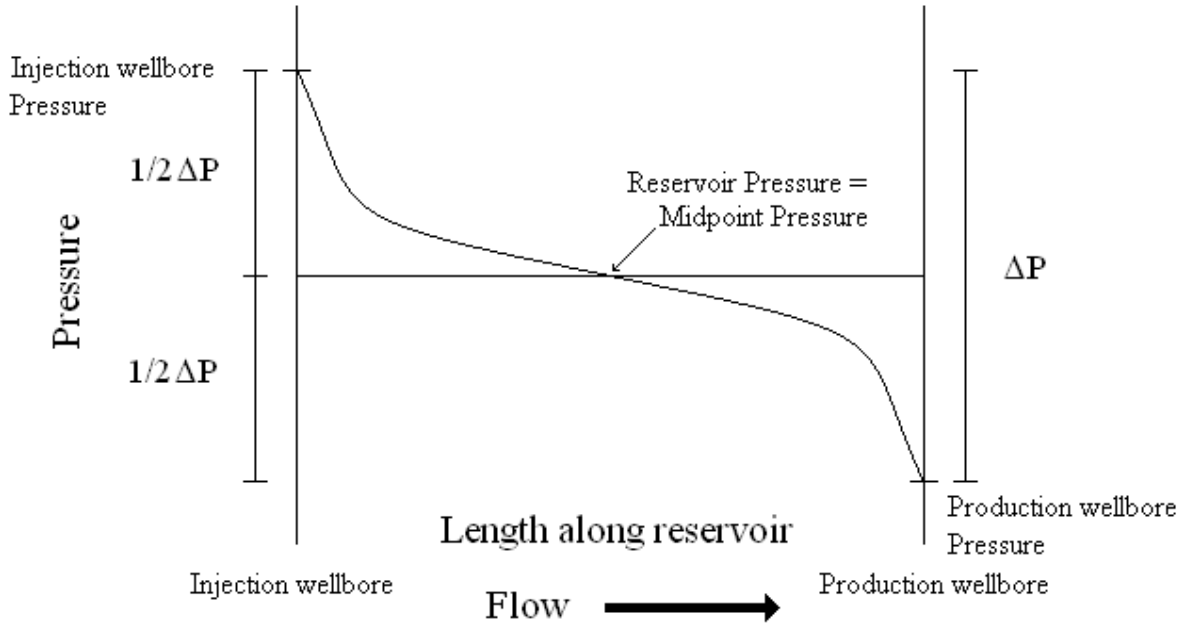


**Figure 5** Reservoir pressure profile assumption described pictorially.

Therefore the required injection pressure at the surface can be calculated by:

$$\Delta P_i = P_i - P_{iw}$$

$$P_i = P_{wi} + \Delta P_i$$

$$P_i = P_r + \frac{\Delta P_r}{2} + \Delta P_i \quad (16)$$

And the resulting production pressure at the surface can be calculated by:

$$\Delta P_p = P_{pw} - P_p$$

$$P_p = P_{pw} - \Delta P_p$$

$$P_p = P_r - \frac{\Delta P_r}{2} - \Delta P_p \quad (17)$$

## Water Properties

The model described above depends significantly on the properties of water, namely density ( $\rho$ ) and viscosity ( $\mu$ ). These properties, particularly viscosity, are highly dependent on temperature and to a lesser extent pressure. The model therefore assumes that water remains at a constant temperature within each section of the model: injection well, fractured reservoir and production well. That is, the water is injected down the injection well at constant temperature  $T_i$ , flows through the reservoir at  $T_r$  and is produced at temperature  $T_p$  in the production well. The pressure acting on the water in the injection well was an average between the required injection pressure and the pressure at the injection wellbore. The pressure of the reservoir,  $P_r$ , was used to determine properties of water within the reservoir, whilst an average between production wellbore pressure and production wellhead pressure was used for calculations concerning the production well.

To determine properties of water at these conditions the Add-In for Microsoft Excel®, *Water97\_v13.xla* (version 1.3) was utilised. This handy Add-In “provides a set of functions for calculating thermodynamic and transport properties of water and steam using the industrial standard IAPWS-IF97” for temperatures of 273.15 to 1073.15 K and pressures of 0 to 1000 bar (Spang 2008). This was consequently incorporated into the Excel program described below. For more information concerning *Water97\_v13.xla* (version 1.3) the reader is directed to <http://www.cheresources.com/iapwsif97.shtml#addin> where it can be downloaded along with its manual.

## Model Limitations

The linear flow equation for fracture flow is derived from an exact solution of the Navier-Stokes equations. However the radial flow equation is derived from an approximate solution to the Navier-Stokes equations for cylindrical coordinates. The model is therefore conceded as approximate.

In addition, the model cannot be applied to turbulent flow regimes within the reservoir. The model is not valid for linear flow if the Reynolds number in that section is greater than 2300. Furthermore turbulence could be likely around the wellbore; the model does not take this into account. However within the radial section, Murphy et al (1978) proposed that laminar flow conditions are expected to be maintained for small radii (that is for around the wellbore) if the

overall Reynolds number  $Re_o = \frac{180q_{pf}\rho}{\pi h\theta\mu} \leq 1.0 \times 10^8$  (Patel & Head 1968). This was purported to

be true, even with local Reynolds numbers well above the usual transitional value, due to stabilising acceleration effects associated with radial flow (Murphy et al 1978).

Thus the model is valid if:

Reynolds in the linear flow section,  $Re_f = \frac{2h\bar{u}\rho}{\mu} \leq 2300$  and overall Reynolds,

$$Re_o = \frac{180q_{pf}\rho}{\pi h\theta\mu} \leq 1.0 \times 10^8 .$$

## Excel Program

The model described above was implemented using Microsoft Excel® so that the required injection pressure, the resulting production pressure and other data could be determined for certain user defined parameters (figure 6). Shown below in figure 7, the program contains a user inputs section (in blue), an outputs section (in yellow), a validity check section (in green) and other calculated data in white. The program starts when the user pushes the start button and then iterates until it converges to within a certain tolerance. The user is able to change the tolerance by: Tools => Options => Calculation, then changing the value in the “maximum change” box. The user is then able to change the inputs in the blue cells of column D and a new answer will be displayed in the large yellow cells. If the inputs are such that the limitations of the model, described above, are breached then the green cells in the validity check section will turn red and display the message “no, change inputs”. This is depicted in figure 8.

	B	C	D	E
1	Well			
2	Inputs			
3	Well Diameter	dw	8	inches
4	Well Depth	D	4500	m
5	Mass Flow Rate	m	100	kg/s
6	Injection Temperature	$T_i$	98	°C
7	Production Temperature	$T_p$	240	°C
8	Reservoir			
9	Inputs			
10	Fracture Aperture	h	0.5	mm
11	Fracture Breadth	w	100	m
12	Distance between wells	L	750	m
13	Number of fractures	n	10	-
14	Angle for Radial Flow	$\theta$	150	°
15	Reservoir Temperature	$T_r$	250	°C
16	Rock Relative Roughness	$\epsilon/h$	0.5	m
17	Reservoir Pressure	$P_r$	10000	psia

Figure 6 User inputs for Excel program.




	B	C	D	E	F	G	H	I					
1	<b>Well</b>				 <table border="1" data-bbox="1003 1066 1154 1740"> <tr> <td>Required Injection Pressure</td> <td>4205.4134</td> <td>psia</td> </tr> <tr> <td>Production Wellhead Pressure</td> <td>4024.1562</td> <td>psia</td> </tr> </table>	Required Injection Pressure	4205.4134	psia	Production Wellhead Pressure	4024.1562	psia		
Required Injection Pressure	4205.4134	psia											
Production Wellhead Pressure	4024.1562	psia											
2	<b>Inputs</b>					Radial Solution Valid?	YES						
3	Well Diameter	dw	8	inches									
4	Well Depth	D	4500	m		Linear Solution Valid?	YES						
5	Mass Flow Rate	m	100	kg/s									
6	Injection Temperature	T <sub>i</sub>	98	°C									
7	Production Temperature	T <sub>p</sub>	240	°C									
8	<b>Reservoir</b>												
9	<b>Inputs</b>												
10	Fracture Aperture	h	0.5	mm									
11	Fracture Breadth	w	75	m									
12	Distance between wells	L	750	m									
13	Number of fractures	n	10	-									
14	Angle for Radial Flow	θ	180	°									
15	Reservoir Temperature	Tr	250	°C									
16	Rock Relative Roughness	z/h	0.5	m									
17	Reservoir Pressure	P <sub>r</sub>	10000	psia									
18	<b>Injection Well Calculated Data</b>												
19	Avg Fluid Density	ρ <sub>avg</sub>	981.539	kg/m <sup>3</sup>	Water Density	ρ	856.4642	kg/m <sup>3</sup>					
20	Avg Fluid Viscosity	μ <sub>avg</sub>	0.0003	kg/m.s	Water Viscosity	μ	1.21E-04	kg/m.s					
21	Avg Fluid Velocity	v <sub>avg</sub>	3.14163	m/s	Flow per fracture	q <sub>f</sub>	0.011676	m <sup>3</sup> /s					
22	Pipe Relative Roughness	z/dw	0.00023	-	External Radius	re	37.5	m					
23	Reynolds Number	Re	2080916	-	Linear Section Length	L'	675	m					
24	Friction Factor	f	0.01452	-	well radius	rw	0.1016	m					
25	Pressure Drop	ΔP	-6058.6	psia	Fracture Aperture (m)	h	0.0005	m					
26	Bottom Hole Pressure	P <sub>z</sub>	10264	psia	<b>Linear Section</b>								
27	Reservoir Pressure Drop	ΔPr	528.032	psia	Fluid Velocity	v	0.311358	m/s					
28	<b>Production Calculated Data</b>				Reynolds Number	Re	2196.10	-					
29	Bottom Hole Pressure	P <sub>s</sub>	9735.95	psia	Friction Factor	f	0.022906	-					
30	Avg Fluid Density	ρ <sub>avg</sub>	852.198	kg/m <sup>3</sup>	Pressure Drop	ΔP	372.3882	psia					
31	Avg Fluid Viscosity	μ <sub>avg</sub>	0.00012	kg/m.s	Pressure Gradient	dp/dL'	0.551686	psia/m					
32	Avg Fluid Velocity	v <sub>avg</sub>	3.61845	m/s	<b>Radial Section</b>								
33	Pipe Relative Roughness	z/dw	0.00023	-	Avg Fluid Velocity	v <sub>avg</sub>	1.17	m/s					
34	Reynolds Number	Re	5156299	-	Reynolds Number	Re <sub>avg</sub>	8286.59	-					
35	Friction Factor	f	0.01425	-	Overall Reynolds	Re <sub>s</sub>	5.24E+07	-					
36	Pressure Drop	ΔP	5711.8	psia	Friction Factor	f <sub>avg</sub>	0.006071	-					
37	Production Well Head P	Pp	4024.16	psia	Pressure Drop	ΔP	77.85174	psia					
38					Pressure Gradient	dp/dr	2.061686	psia/m					


Figure 7 Screen print out of Excel program.

	F	G	H	I	
1					
2					
3					
4		<b>Required Injection Pressure</b>	<b>4256.955</b>	<b>psia</b>	
5					
6					
7					
8			<b>Production Wellhead Pressure</b>	<b>3973.272</b>	<b>psia</b>
9					
10					
11	<b>Radial Solution Valid?</b>		<b>NO, Change Inputs</b>		
12					
13					
14	<b>Linear Solution Valid?</b>		<b>YES</b>		
15					
16					

(a)

	F	G	H	I	
1					
2					
3					
4		<b>Required Injection Pressure</b>	<b>4978.737</b>	<b>psia</b>	
5					
6					
7					
8			<b>Production Wellhead Pressure</b>	<b>3261.154</b>	<b>psia</b>
9					
10					
11	<b>Radial Solution Valid?</b>		<b>YES</b>		
12					
13					
14	<b>Linear Solution Valid?</b>		<b>NO, Change Inputs</b>		
15					
16					

(b)

	F	G	H	I	
1					
2					
3					
4		<b>Required Injection Pressure</b>	<b>5296.153</b>	<b>psia</b>	
5					
6					
7					
8			<b>Production Wellhead Pressure</b>	<b>2948.265</b>	<b>psia</b>
9					
10					
11	<b>Radial Solution Valid?</b>		<b>NO, Change Inputs</b>		
12					
13					
14	<b>Linear Solution Valid?</b>		<b>NO, Change Inputs</b>		
15					
16					

(c)

**Figure 8** Excel program output for (a) invalid radial solution (b) invalid linear solution and (c) both linear and radial invalid.

## Sensitivity Analysis

Using the program created in Excel the model was put through a series of sensitivity analyses where the impact of different input variables was assessed. The parameters to be tested were:

### Mass Flow Rate Analysis

The required mass flow rate for effective heat extraction in a geothermal reservoir is expected to be between 75 and 100kg/s.

Tested for impact on:

- required injection pressure/resulting production pressure at the surface;
- reservoir pressure profile; and
- reservoir pressure drop

### Fracture Aperture Analysis

Fracture aperture is critical in fracture fluid flow as demonstrated from the cubic law (see appendix).

Tested for impact on:

- required injection pressure/resulting production pressure at the surface;
- reservoir pressure profile;
- reservoir pressure drop; and
- model validity

### Fracture Width Analysis

Fracture width, according to the model, impacts on the range of radial and linear flow within a fracture. Tested for impact on:

- required injection pressure/resulting production pressure at the surface;
- reservoir pressure profile;
- reservoir pressure drop; and
- model validity

### Number of Fractures Analysis

The flow of water through each fracture in this model was assumed equal due to each having identical geometry. The number of fractures therefore would impact on not only the pressure drop in the reservoir but also the validity of the model, as Reynolds and overall Reynolds are directly proportional to fracture flow.

Tested for impact on:

- required injection pressure/resulting production pressure at the surface;
- reservoir pressure profile;
- reservoir pressure drop; and
- model validity

## Roughness Analysis

Roughness creates a friction element that impedes fracture flow.

Tested for impact on

- deviations from the cubic law

## Reservoir Temperature Analysis

The reservoir temperature affects the properties of water, in particular viscosity.

Tested for impact on:

- required injection pressure/resulting production pressure at the surface;
- reservoir pressure profile; and
- reservoir pressure drop

## Results

NB: each analysis was evaluated for a single fracture zone of depth 4500m and well diameter of 8 inches.

### Mass Flow Rate

Figure 9 displays the impact that mass flow rate has on required injection pressure/resulting production pressure at the surface.

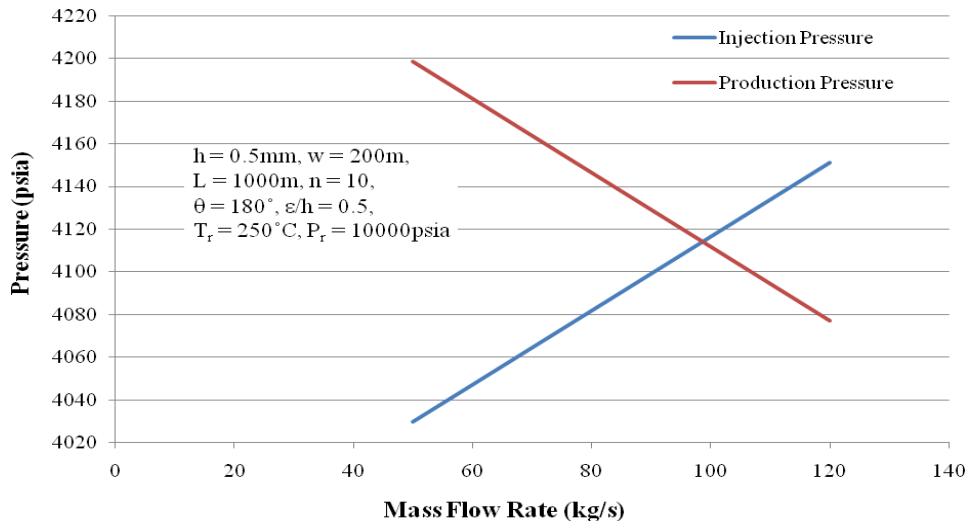


Figure 9 Effect of mass flow rate on required injection pressure and resulting production pressure.

Figure 10 demonstrates the effect of mass flow rate on the reservoir pressure profile.

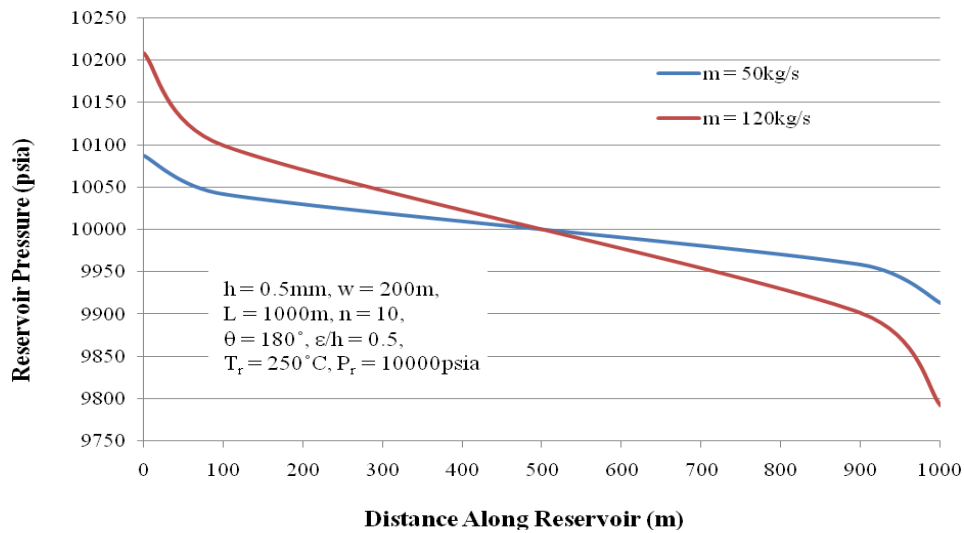


Figure 10 Effect of mass flow rate on reservoir pressure profile.

Figure 11 depicts the impact of mass flow rate on reservoir pressure drop.

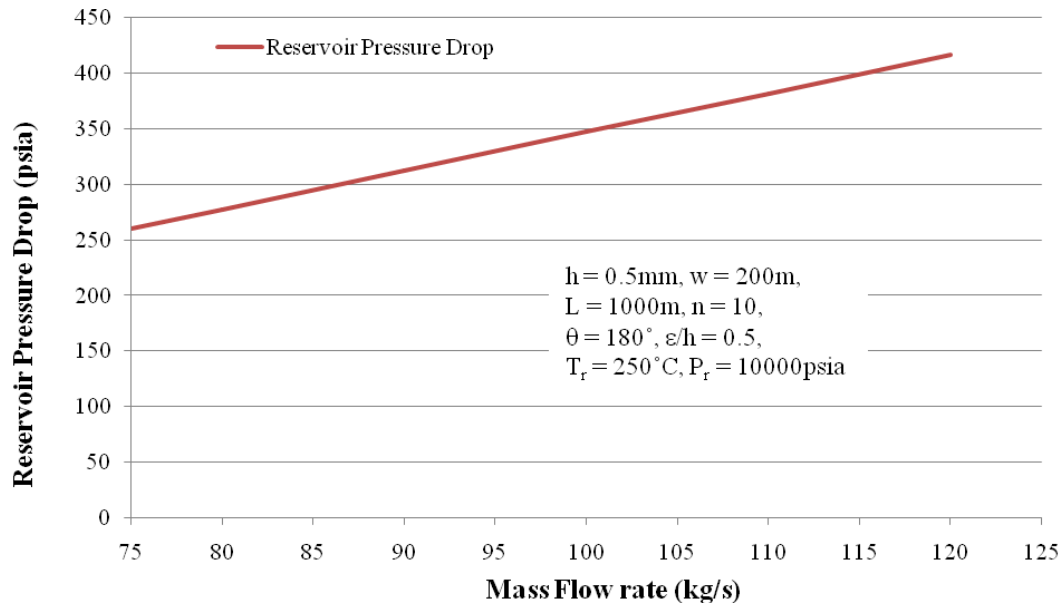


Figure 11 Effect of mass flow rate on reservoir pressure drop.

### Fracture Aperture

Figure 12 demonstrates the impact of fracture aperture on both required injection pressure and resulting production pressure at the surface.

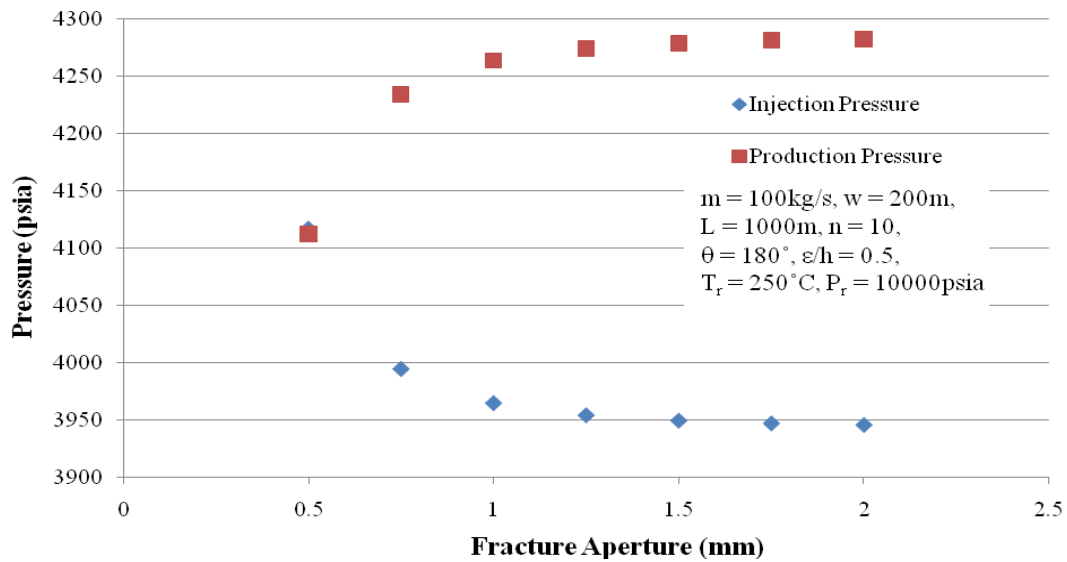


Figure 12 Impact of fracture aperture on required injection pressure and production pressure.

Figure 13 displays the effect of fracture aperture on reservoir pressure profile.

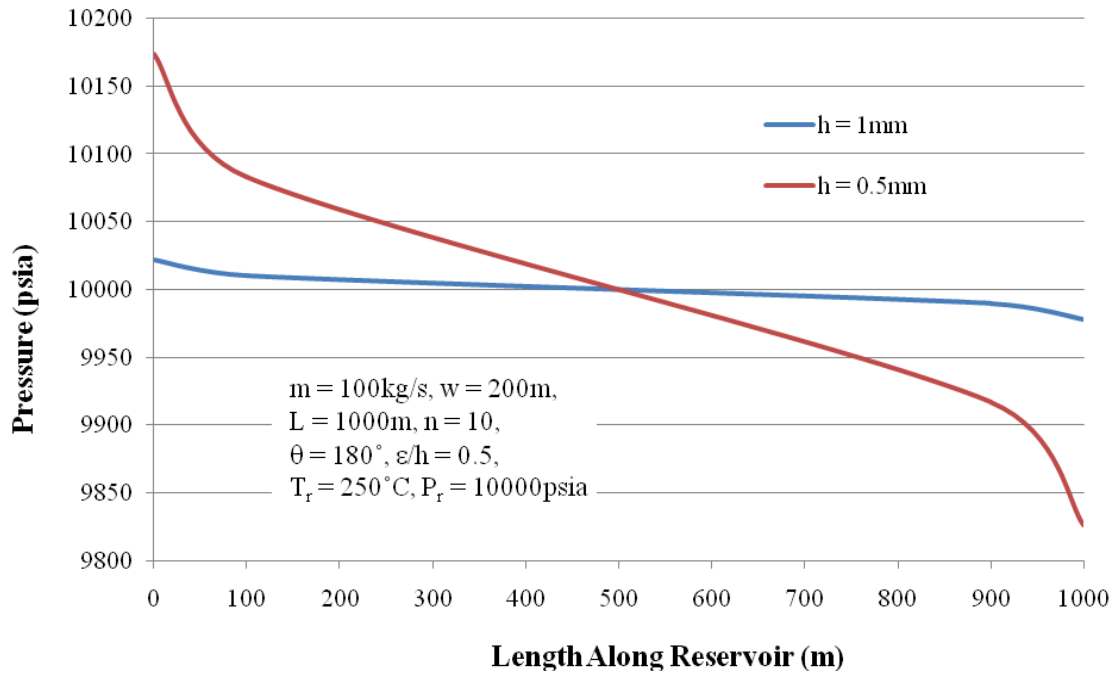


Figure 13 Effect of fracture aperture on reservoir pressure profile.

Figure 14 depicts the impact of fracture aperture on reservoir pressure drop.

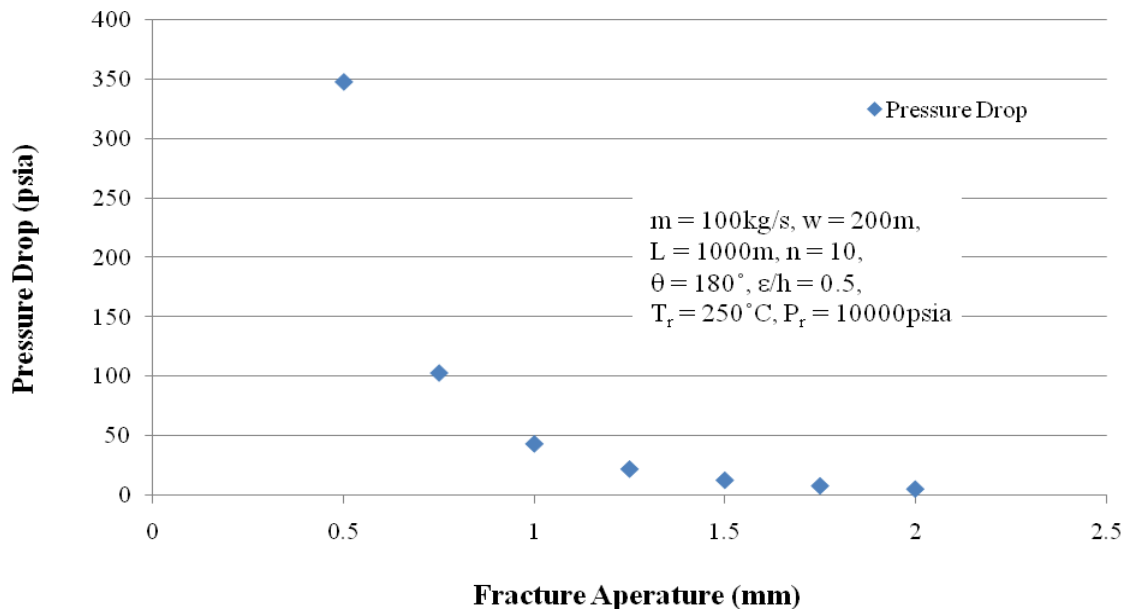


Figure 14 Effect of fracture aperture on reservoir pressure drop.

Figure 15 shows the ranges of fracture aperture for which the model has a valid radial solution.

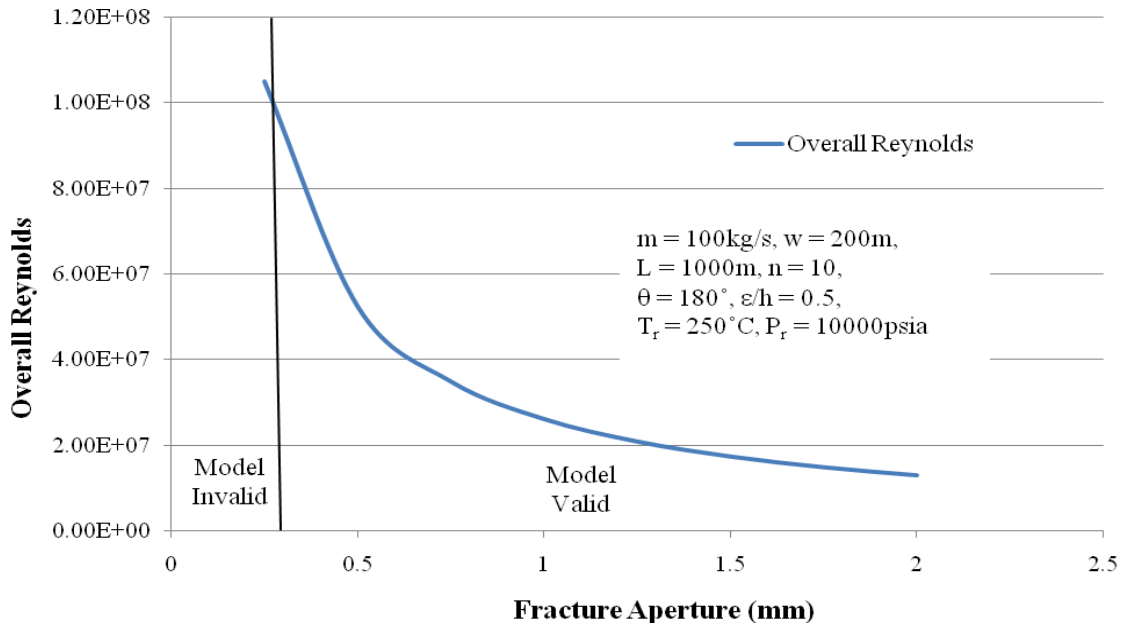


Figure 15 Model radial solution validity for fracture aperture.

### Fracture Width

Figure 16 displays the effect of fracture width on required injection pressure and resulting production pressure at the surface.

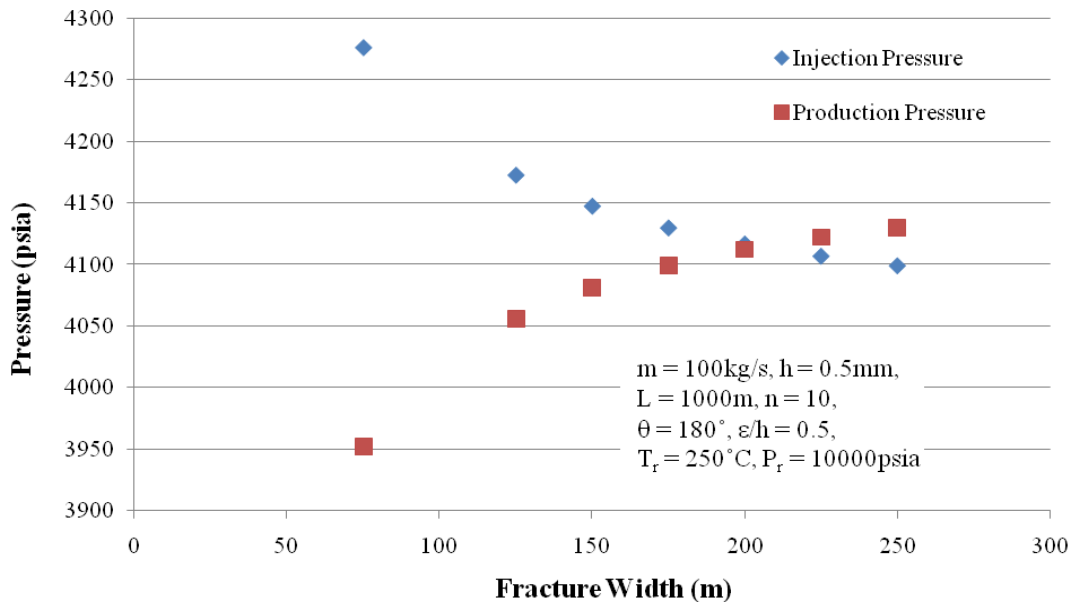


Figure 16 Effect of fracture width on required injection pressure and resulting production pressure.

Figure 17 shows the impact of fracture width on reservoir pressure profile.

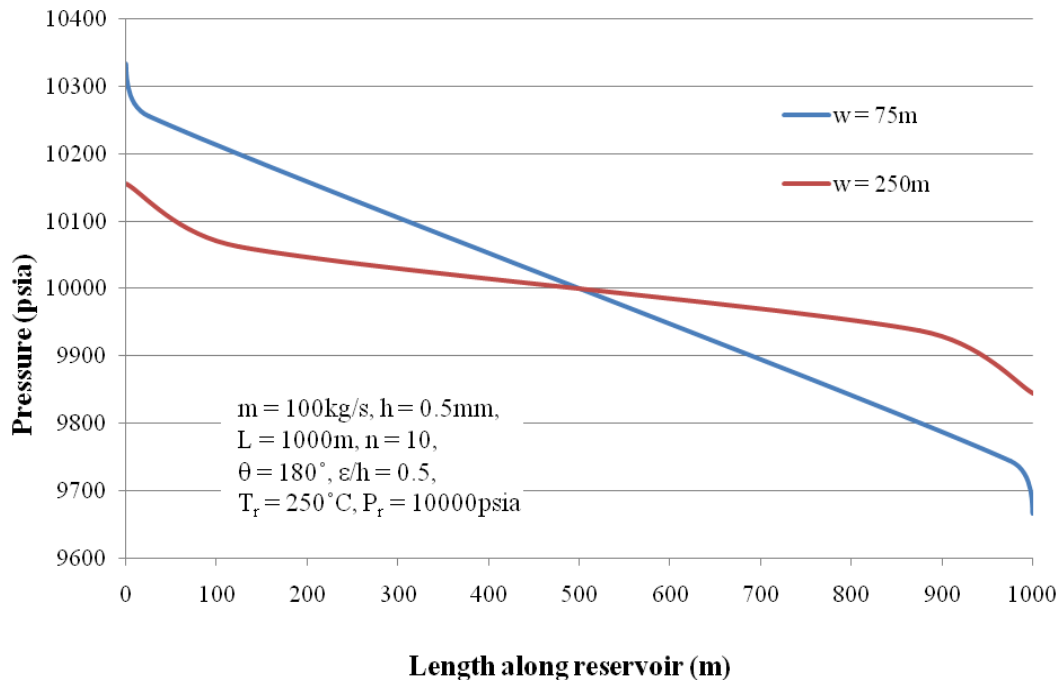


Figure 17 Impact of fracture width on reservoir pressure profile.

Figure 18 depicts the effect of fracture width on reservoir pressure drop.

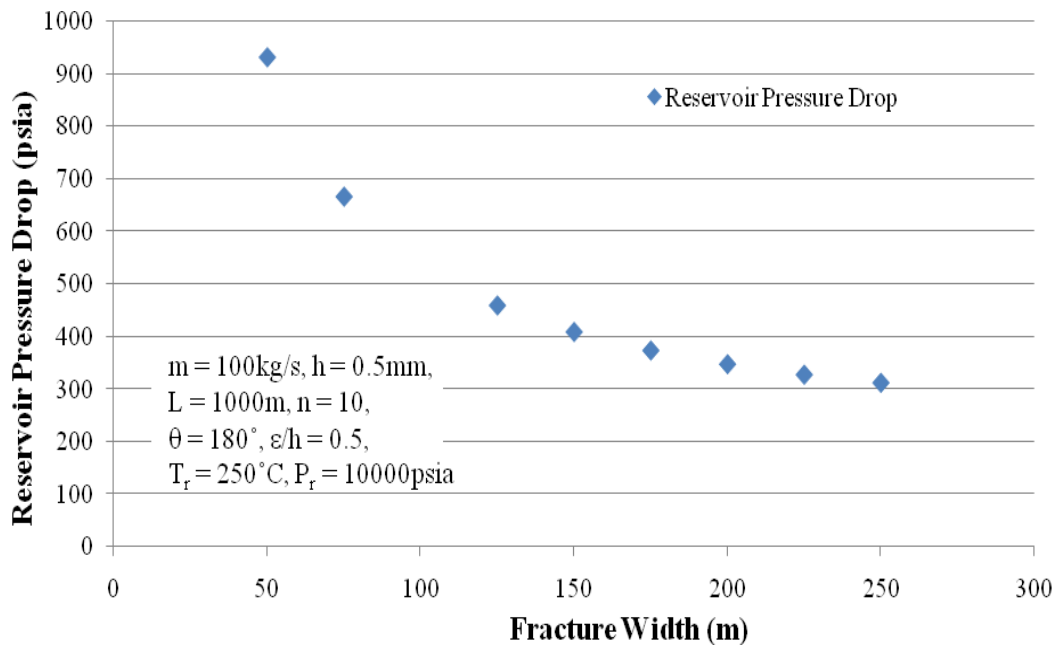


Figure 18 Effect of fracture width on reservoir pressure drop.

Figure 19 demonstrates the effect of fracture width on model linear solution validity.

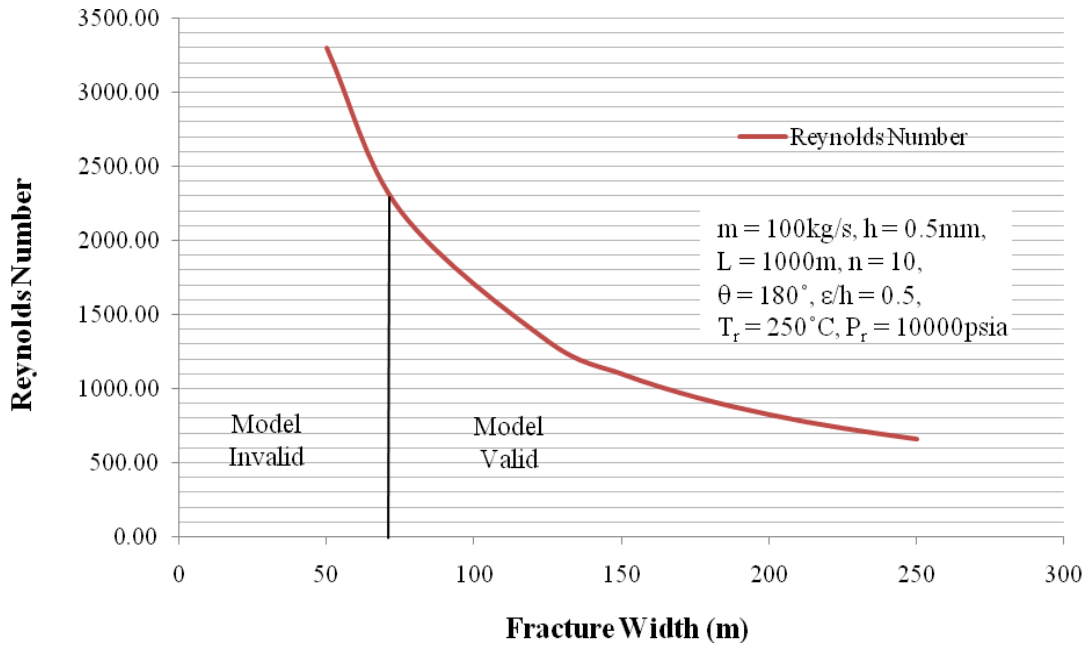


Figure 19 Impact of fracture width on model linear solution validity.

### Number of Fractures

Figure 20 displays how required injection pressure and resulting production pressure at the surface were affected by number of fractures.

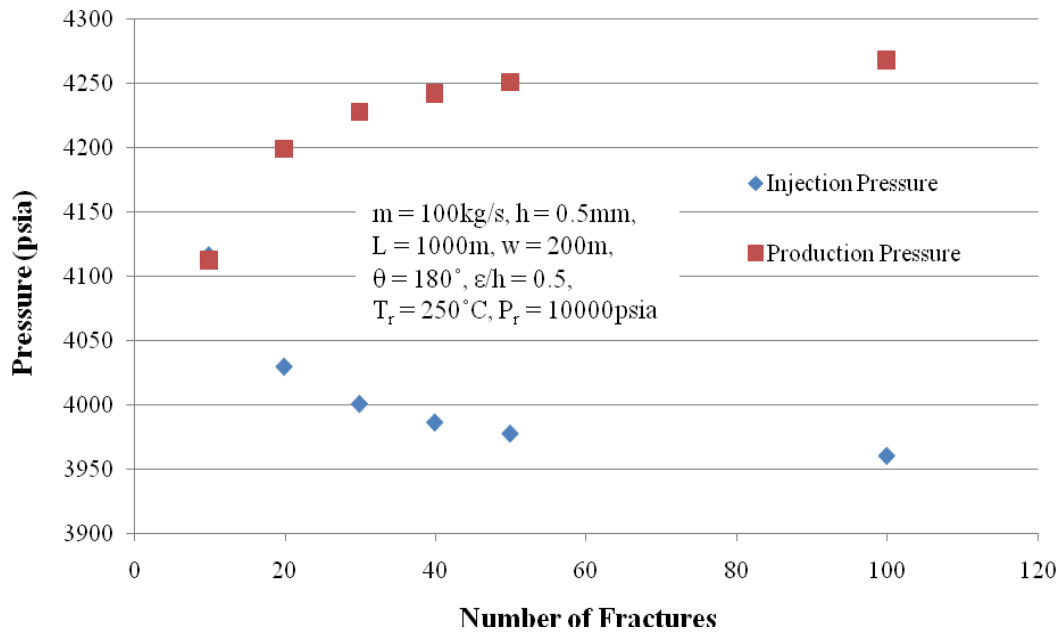


Figure 20 Impact of number of fractures on required injection pressure and resulting production pressure.

Figure 21 demonstrates the impact of number of fractures on reservoir pressure profile.

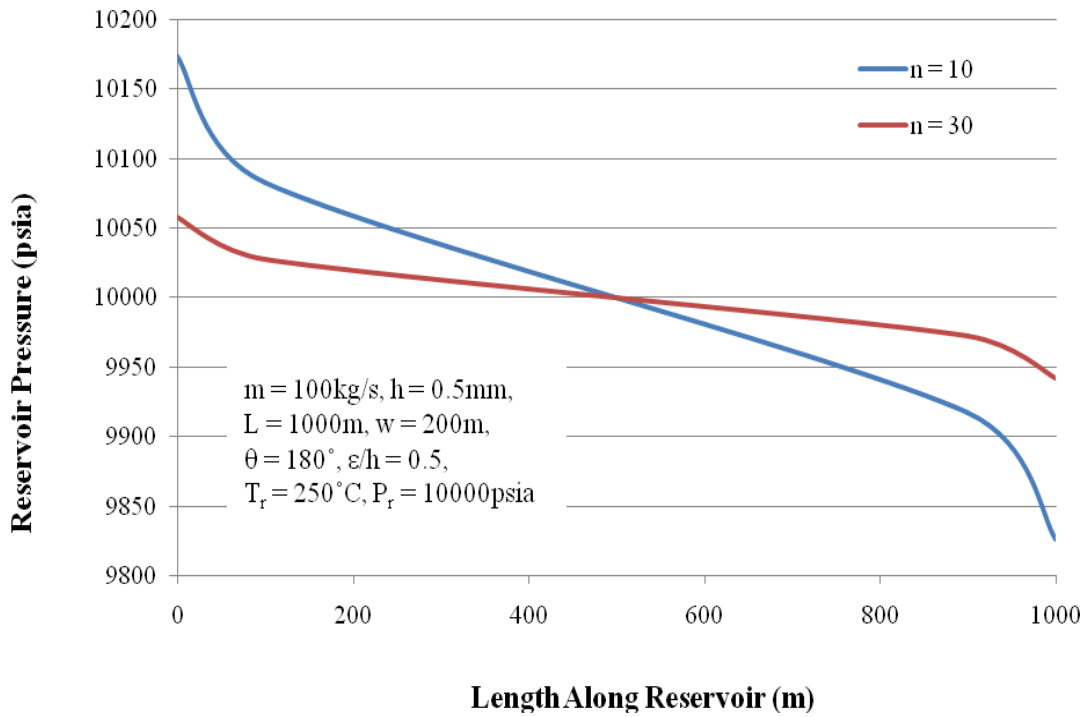


Figure 21 Effect of number of fractures on reservoir pressure profile.

Figure 22 depicts the impact of number of fractures on reservoir pressure drop.

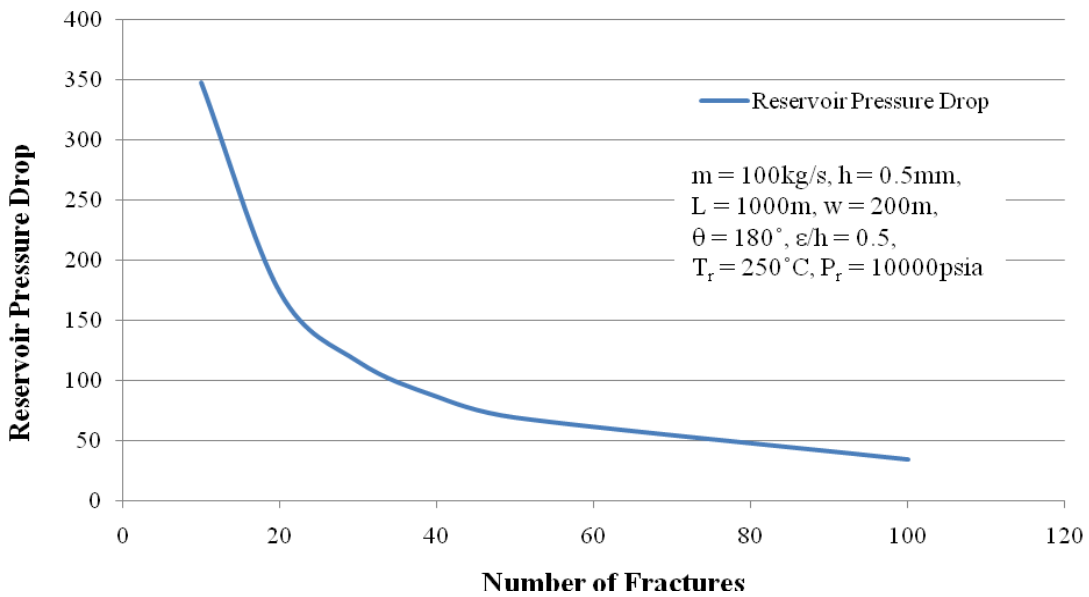


Figure 22 Effect of number of fractures on reservoir pressure drop.

Figure 23 displays how the validity of the model is affected by the number of fractures.

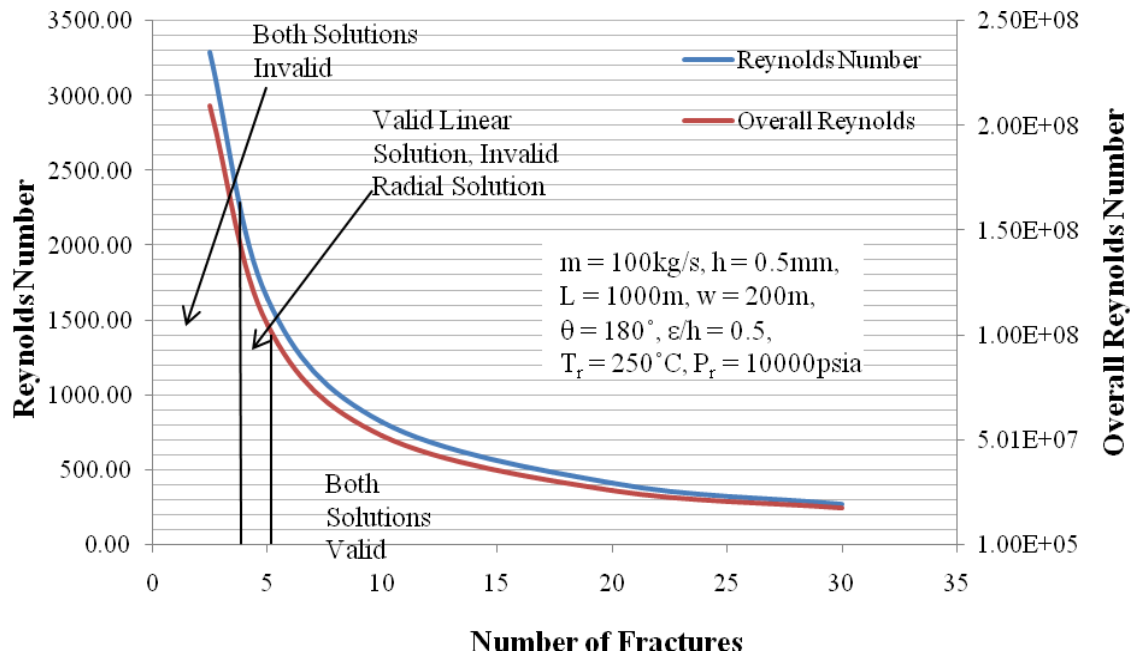


Figure 23 Impact of number of fractures on model validity.

### Roughness

Figure 24 shows the impact of rock roughness on reservoir pressure drop and the deviation of the model from the cubic law.

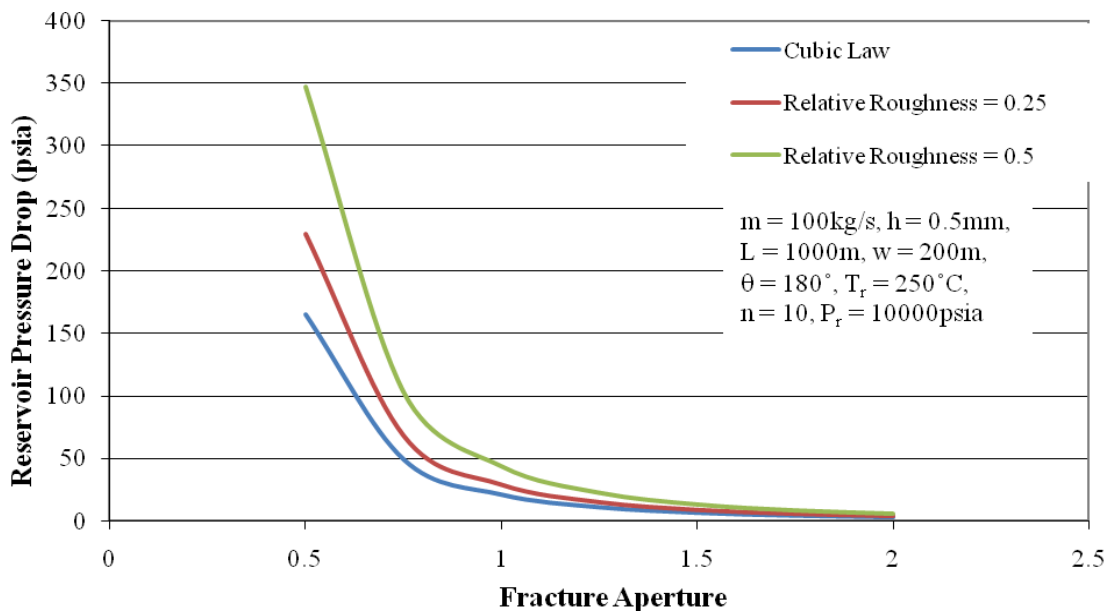
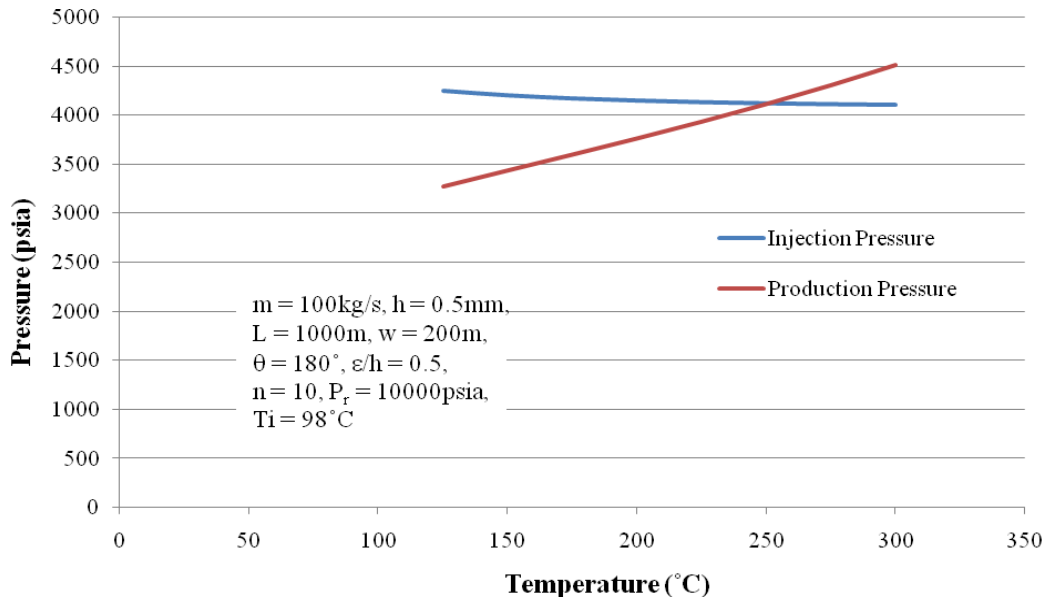


Figure 24 Effect of rock roughness on reservoir pressure drop.

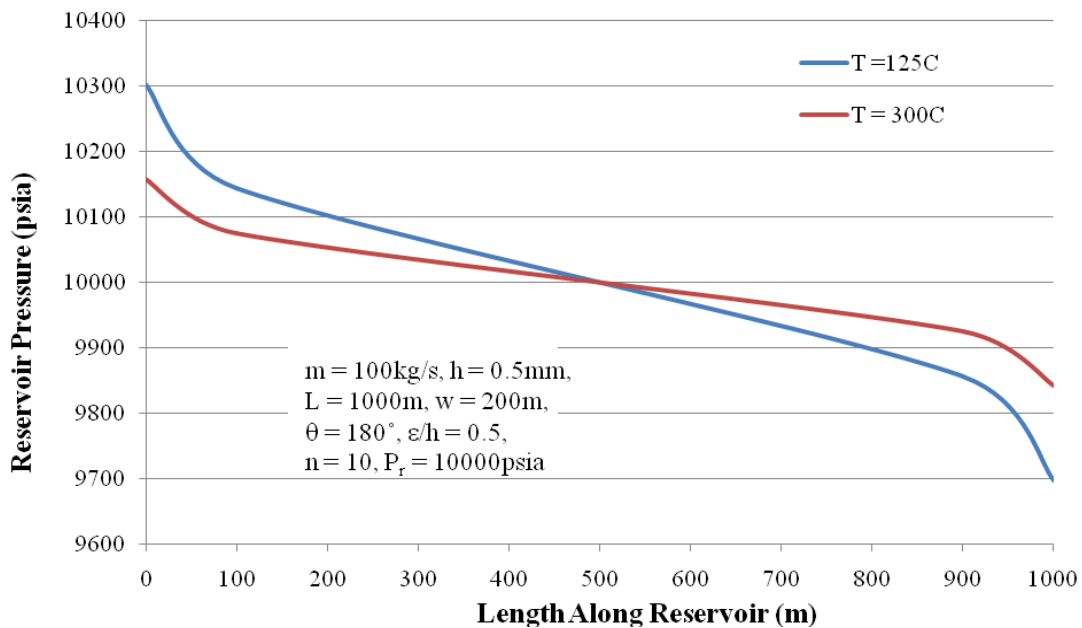
## Reservoir Temperature

Figure 25 shows how required injection pressure and resulting production pressure at the surface vary with reservoir temperature.



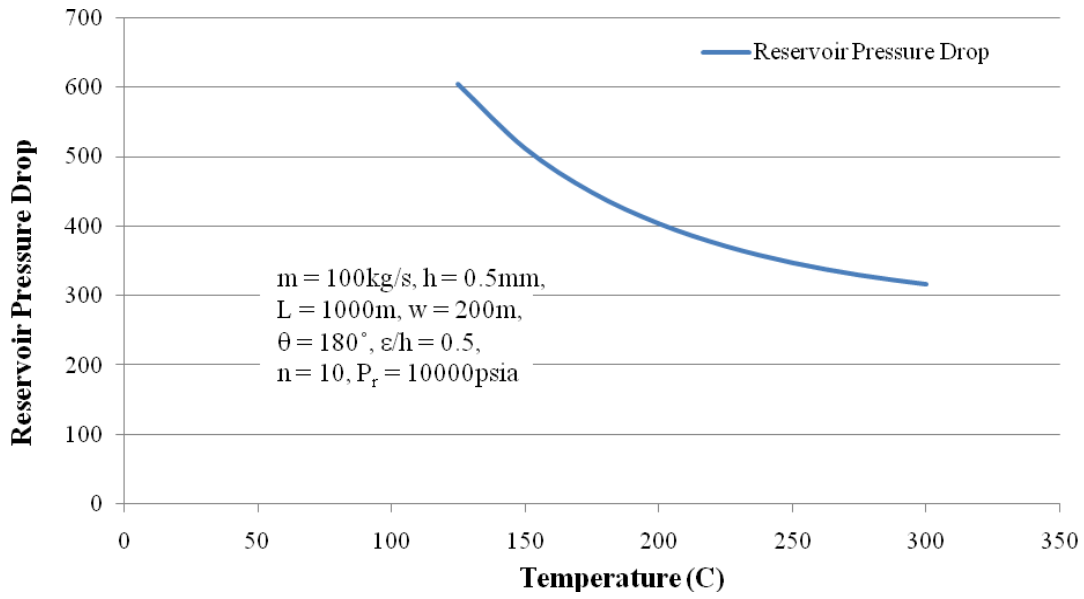
**Figure 25** Effect of reservoir temperature on required injection pressure and resulting production pressure.

Figure 26 demonstrates the effect of reservoir temperature on reservoir pressure profile.



**Figure 26** Effect of reservoir temperature on reservoir pressure profile.

Figure 27 displays the effect of reservoir temperature on reservoir pressure drop.



**Figure 27** Change of reservoir pressure drop with reservoir temperature.

## Discussion

### Required injection pressure and resulting production pressure

The results of this analysis for variables mass flow rate, fracture aperture, fracture width, number of fractures and reservoir temperature are displayed in figures 9, 12, 16, 20 and 25 respectively. These figures are significant because they show the point where production pressure begins to exceed injection pressure. A geothermal system will be most efficient when production pressure exceeds injection pressure, as this allows for some pressure drop to occur along the electricity production process. If production pressure is lower than the required injection pressure then extra power is required to pump the flow up to the reinjection pressure. This may make the geothermal system redundant if it ends up consuming more energy than it creates. The model is thus useful for determining how much pressure, if any, can be expended during the electricity production process.

One finding from this analysis is that the production pressure begins to exceed the injection pressure before reservoir pressure drop approaches zero. This is interesting because the hydrostatic pressure resulting from vertical displacement was expected to cancel out. However it was found that production pressure exceeded required injection pressure for many reservoir geometries which had non-zero reservoir pressure drop solutions. The reason for this is that the water in the production well is less dense and less viscous than the water in the injection well, due to higher temperatures, and thus flows with less pressure drop. Hydrostatic pressure is equal to  $\rho g(z_1 - z_2)$ , which means that the less dense water in the production well flows against less hydrostatic pressure than the amount that is gained by the water in the injection well. The consequence of this finding is that it may be possible to operate a geothermal power plant as a closed system. That is, the production pressure may be high enough such that even after allowing for the prescribed pressure drop across the electricity production process, flow pressure is still high enough for reinjection into the reservoir.

This finding is best described mathematically:

As  $\Delta P_r \rightarrow 0$ ,  $P_i \rightarrow P_r + \Delta P_i$  and  $P_p \rightarrow P_r - \Delta P_p$

And for  $T_p > T_i$ ,  $\Delta P_p < -\Delta P_i$ , due to water being less dense and less viscous in the production well

NB: negative in front of  $\Delta P_i$  is to make it a positive pressure drop. The hydrostatic pressure gain is larger than the friction losses in the injection well hence  $\Delta P_i$  is always negative.

Hence letting  $P_i - P_r - \Delta P_i = 0$  and letting  $P_p - P_r + \Delta P_p = 0$  and equating these two expressions:

$$P_i - P_r - \Delta P_i = P_p - P_r + \Delta P_p$$

$$P_p - P_i = -\Delta P_i - \Delta P_p$$

And since  $\Delta P_p < -\Delta P_i \therefore -\Delta P_i - \Delta P_p > 0$  and  $\therefore P_p - P_i > 0$

$\therefore P_p > P_i$

Hence much depends on reducing reservoir pressure drop if a closed EGS is to be achieved. The effect of each parameter on reservoir pressure drop is discussed below.

## Reservoir Pressure Profile

The reservoir pressure profile analysis for mass flow rate, fracture aperture, fracture width, number of fractures and reservoir temperature are shown in figures 10, 13, 17, 21 and 26 respectively. The purpose of this analysis was to demonstrate the effect of each parameter on reservoir pressure drop in a way that would also describe the effect of those parameters on wellbore pressure. The above-mentioned figures have on the horizontal axis “length along reservoir”, 0m being the location of the injection wellbore and 1000m being the location of the production wellbore. Thus the plots show what the pressure of flow is at any point along the reservoir. It should be noted that the midpoint pressure of the reservoir is equal the reservoir pressure. This stems from the assumption made for this model that the injection wellbore pressure must be equal to the reservoir pressure plus half the reservoir pressure drop in order to achieve flow into the reservoir, and that the production wellbore pressure must be equal to the reservoir pressure minus the other half of reservoir pressure drop in order to achieve flow into the production wellbore (figure 5).

It can be seen that the slope of the pressure profile increases at each end of the plots whilst in the middle slope remains steady. This occurs due to the fractures being split into a radial section followed by a linear section followed by another radial section, and equations 10 and 11 that show reservoir pressure drop in proportion with fluid velocity squared. In the linear section fluid velocity is constant due to a constant cross-sectional area. However in radial flow the velocity increases rapidly as the wellbore is approached. Thus the average velocity in the radial section will always be larger than in the linear section. Therefore the pressure gradient in the radial sections is always steeper than in the linear section. The plots from this analysis also show then the point along the fracture where the flow regime changes from radial to linear and back to radial again.

## Reservoir Pressure Drop

The results from the sensitivity analysis on reservoir pressure drop are shown below in table I.

**Table I** Results summary from reservoir pressure drop sensitivity analysis.

Tested Variable	Symbol	Influence on Pressure Drop
Mass flow rate	m	Directly proportional, $\Delta P \uparrow$ as m $\uparrow$
Fracture aperture	h	Inversely proportional to some power, $\Delta P \downarrow$ as h $\uparrow$
Fracture width	w	Inversely proportional, $\Delta P \downarrow$ as w $\uparrow$
Number of fractures	n	Inversely proportional, $\Delta P \downarrow$ as n $\uparrow$
Rock roughness	$\epsilon$	Proportional to some power, $\Delta P \uparrow$ as $\epsilon \uparrow$
Reservoir temperature	$T_r$	Inversely proportional, $\Delta P \downarrow$ as $T_r \uparrow$

The results of the sensitivity analysis were simply direct consequences of the mathematics of the model. However the purpose of the analysis was to illustrate the effect of each parameter on

pressure drop more clearly to the reader. The effect of each parameter can also be demonstrated simply by expanding the pressure drop equations:

$$\Delta P_{in} = f\rho \frac{L'}{h} \hat{u}^2 = \frac{24}{\text{Re}} \left( 1 + 3.1 \left( \frac{\varepsilon}{h} \right)^{1.5} \right) \rho \frac{L'}{h} \hat{u}^2$$

$$\Delta P_{in} = \frac{24\mu}{2\rho\hat{u}h} \left( 1 + 3.1 \left( \frac{\varepsilon}{h} \right)^{1.5} \right) \rho \frac{L'}{h} \hat{u}^2$$

$$\Delta P_{in} = \frac{12\mu L' \hat{u}}{h^2} \left( 1 + 3.1 \left( \frac{\varepsilon}{h} \right)^{1.5} \right)$$

$$\Delta P_{in} = \frac{12\mu L' q_{pf}}{h^3 w} \left( 1 + 3.1 \left( \frac{\varepsilon}{h} \right)^{1.5} \right)$$

$$\Delta P_{in} = \frac{12\mu L' m}{h^3 w n \rho} + \frac{37.2\mu L' m \varepsilon^{1.5}}{h^{4.5} w n \rho}$$

And similarly for radial flow (for an entire circle):

$$\Delta P_{rad} = f\rho \frac{(r_e - r_w)}{h} \hat{u}^2 \quad \Rightarrow \quad \Delta P_{rad} = \frac{6m\mu \ln\left(\frac{r_e}{r_w}\right)}{h^3 \pi m \rho} + \frac{18.6m\mu \ln\left(\frac{r_e}{r_w}\right) \varepsilon^{1.5}}{h^{4.5} \pi m \rho}$$

These expanded expressions further explain the results of the sensitivity analysis. Total mass flow rate is directly proportional to pressure drop and thus produced a linear plot in figure 11. Number of fractures and fracture width are inversely proportional to pressure drop so hence formed plots that decreased along the horizontal axis in figures 22 and 18 respectively.

Reservoir temperature is the only parameter that cannot be seen in the above expressions. However, the parameters of density and viscosity are functions of temperature and are present in the expanded expressions. Thus it can be seen that reservoir temperature is important for two reasons. First, increasing temperature causes viscosity to decrease and thus causes pressure drop to decrease, as it is directly proportional. Second, density decreases as temperature increases, which causes pressure drop to increase as  $\rho$  is inversely proportional. However, figure 27 indicates that pressure drop decreases with increasing temperature. Thus viscosity is more sensitive to temperature than density and this can be seen in appendix C.

Rock roughness was important to analyse because it demonstrates the model's deviation from the cubic law at small apertures. The cubic law is traditionally used to describe flow between smooth parallel plates but in fracture flow, rock surfaces contain an element of roughness. The first term in each of the expanded expressions above is the cubic law for linear and radial flow, whilst the second term incorporates rock roughness. The effect of the second term can be seen in figure 24 which plots the cubic law along with 25 and 50% relative roughness on a plot of pressure drop

versus fracture aperture. Figure 24 demonstrates that for small apertures, reservoir pressure drop increases significantly with increasing rock roughness. This is reinforced by the expressions above that show roughness proportional to the power 1.5. It should be noted that the  $\varepsilon^{1.5}$  term is empirically derived from experiments by Louis (1969).

Fracture aperture was determined to be a very influential parameter of the model. Figure 14 is particularly effective in demonstrating the dramatic decrease in pressure drop with increasing aperture. This result is logical. If water has more space to flow through, then there will be less resistance to flow and hence less pressure drop. However the extent of aperture's influence is realised more when one observes the pressure drop expressions above. In the traditional cubic law term fracture aperture is inversely proportional to pressure drop to the power 3 (hence the cubic law), and in the roughness term fracture aperture is inversely proportional to the power 4.5. This leads to the finding that fracture aperture is perhaps the most important element of a geothermal reservoir, and emphasises the need to hydraulically fracture hot rock before a reservoir can be effectively utilised.

### Model Validity

This analysis was conducted for fracture aperture, fracture width and number of fractures, the results for which are shown in figures 15, 19 and 23 respectively. The purpose of this analysis was to demonstrate the limitations of the model. Figure 15 contains the overall Reynolds number only as the local Reynolds number in the linear section is not actually affected directly by fracture aperture. This can be shown mathematically:

$$\text{Re} = \frac{2h\hat{u}\rho}{\mu}$$

$$\text{But } \hat{u} = \frac{q_{pf}}{A} = \frac{q_{pf}}{wh}$$

$$\therefore \text{Re} = \frac{2hq_{pf}\rho}{wh\mu} = \frac{2q_{pf}\rho}{w\mu}$$

Similarly figure 19 only contains the local Reynolds number as the overall Reynolds number only concerns radial flow and is not at all dependent on fracture width (see appendix A). Figure 23 however contains both Reynolds numbers as the number of fractures determines the volumetric flow rate through each fracture. Given that both Reynolds numbers are dependent on flow rate a model validity analysis could have been conducted on mass flow rate. However for the parameters that defined the analysis on mass flow rate, no invalidity was found. Invalidity would have occurred for higher flow rates of around 200kg/s. However economic flow rates for geothermal reservoirs of the type modelled in this study are only in the range of 50 to 100kg/s (Massachusetts Institute of Technology 2006).

The results of the model validity analysis show that the range of invalidity for each parameter was relatively small. Figure 15 shows that the model was only invalid for fracture aperture less than 0.3mm, whilst figure 19 demonstrates that the model is only invalid for fracture widths less than approximately 70m. Figure 23 illustrates that invalidity occurs only when there is less than approximately 5 fractures of 0.5mm aperture and 200m width. These ranges could be considered uneconomical reservoir geometries. Five and even ten fractures of aperture 0.2 to 0.5mm in a

reservoir would not be considered favourable. The model is therefore valid for geometries that are commercially viable and thus could have industrial applicability.

It should be noted that for linear flow the model uses the traditional critical Reynolds number for pipe flow of 2300. This means that for flow in the linear section, if the Reynolds number is greater than 2300 then turbulent flow occurs. However Jones et al (1988) determined that for rough fractures of small aperture (less than 0.6mm) the critical Reynolds number may be 600 or lower. If the model were to take this approach, it is unlikely that it would be valid for many scenarios without a method for modelling turbulent flow. Louis (1969), in addition to the friction factor used in this study, did develop a turbulent friction factor for flow in natural fractures. However during the development of this model, difficulties were experienced when attempting to account for turbulence in the radial flow section around the wellbore. Hence the model only accounts for laminar flow in the reservoir.

### Recommendations

This model is simplistic in terms of reservoir geometry. Geothermal reservoirs are unlikely to consist of perfectly horizontal fractures of identical width and constant aperture. In the real world fractures are tortuous, interconnected, and would perhaps not all communicate wellbore to wellbore. However this model does allow for quick approximation of pressure data from injection wellhead to production wellhead providing a “best case scenario” solution. And despite the simplistic nature of the model it is a good basis for further development and sophistication. Therefore it is recommended that additional elements such as multiple fracture zones, fracture interconnection, varying fracture orientation, non-identical fractures and tortuous flow path should be implemented into the model geometry. These elements would make the model more realistic.

A more accurate solution to the radial flow problem should be researched in order to make the model more precise. In addition the effects of turbulence around the wellbore should be further investigated. This would improve not only the overall precision of the model but also its applicability.

The model should also be extended and incorporate the power plant on the surface. This would complete the model as a steady-state geothermal system and allow for further understanding as to the feasibility and potential of geothermal energy in the Cooper Basin.

The recommendation for the long term is to convert the model from steady-state to transient in order to incorporate time factors such as reservoir cooling, rock/pipe/heat exchanger fouling and rock erosion and deformation. This would enlighten the long-term potential of geothermal energy as a sustainable energy source.

## Conclusions

- The model showed that, for given reservoir geometries, it is possible for resulting production pressure to exceed required injection pressure. This was reasoned to be the result of less dense and less viscous water flowing in the production well than in the injection well. This means that it may be possible to operate a geothermal power plant as a closed system.
- The reservoir pressure profile plots showed that the larger pressure drops within the reservoir occur at the wellbores where the flow regime is radial.
- The sensitivity analysis on reservoir pressure drop demonstrated that fracture aperture is the most important element of a geothermal reservoir with respect to flow. This can also be shown by expansion of the reservoir pressure drop equations into the cubic law and the roughness term.
- The model was found to be applicable to many reservoir geometries. It was invalid for a relatively small range and only for undesirable reservoir geometries. However it was conceded that the critical Reynolds number could be lower than the one used in the linear section of the model, as proposed in a study by Jones et al (1988).
- The model was conceded as simplistic but it is a good basis for further sophistication and refinement.
- It was recommended that the geometry of the model be altered to incorporate additional elements such as multiple fracture zones, fracture interconnectivity, varying fracture orientation and tortuous flow path.
- A more accurate solution to the Navier-Stokes radial flow equation should be sought and the effect of turbulent flow around the wellbore should be further investigated in order to make the model more precise and applicable.
- In order to complete the model it should be extended to include to surface power plant that would be situated between wellheads.
- The long-term recommendation was that the model be converted from steady-state to transient in order to further understand the potential of geothermal energy in South Australia.

## Nomenclature

<b>Symbol</b>	<b>Meaning</b>	<b>Units</b>
A	Area	m <sup>2</sup>
c <sub>p</sub>	Specific heat capacity	J/kg.K
D	Well depth	m
ΔP	Pressure drop	psia
d <sub>w</sub>	Well diameter	m
ε	Roughness	m
f	Friction factor	-
g	Gravitational acceleration	9.81 m/s <sup>2</sup>
h	Fracture aperture	m
h <sub>L</sub>	Energy loss	m <sup>2</sup> /s <sup>2</sup>
ĥ	Heat transfer coefficient	W/m <sup>2</sup> .K
k	Thermal conductivity	W/m.K
L	Distance between wells	m
L'	Length of linear flow section	m
m	Total mass flow rate	kg/s
Nu <sub>T</sub>	Nusselt number at constant temperature	-
μ	Fluid dynamic viscosity	Pa.s
n	Number of fractures	-
ν	Kinematic viscosity	m <sup>2</sup> /s
P	Pressure	Psia
Q	Heat flow	W
q	Volumetric flow rate	m <sup>3</sup> /s
θ	Angle of radial flow	°
Re	Reynolds number	-
r	Radius/cylindrical coordinate in the r direction	m
ρ	Fluid density	kg/m <sup>3</sup>
σ	Cylindrical coordinate in the σ direction	m
T	Temperature	°C
t	Time	s
u	Velocity in the x direction	m/s
û	Average velocity	m/s
v	Velocity in the y direction	m/s
w	Fracture width/velocity in the z direction	m
z	Vertical Displacement/Cartesian and cylindrical coordinate	m
<b>Subscripts</b>		
avg	Average	
b	Bulk	
e	External	
f	Fracture	
i	Injection	
lin	Linear flow	
o	Overall	
0	Initial	
p	Production	
pf	Per fracture	
rad	Radial flow	
r	Reservoir	
w	Well	

## Conversion Factors

<b>Convert</b>	<b>From</b>	<b>To</b>	<b>Multiply by</b>
Density	lb/ft <sup>3</sup>	kg/m <sup>3</sup>	$1.602 \times 10^1$
Length	ft	m	$3.048 \times 10^{-1}$
	in	m	$2.54 \times 10^{-2}$
Mass	lb	kg	$4.536 \times 10^{-1}$
Pressure	psia	Pa	$6.895 \times 10^3$
Temperature	°F	°C	$T_C = (5/9)(T_F - 32^\circ)$
Viscosity	lb.s/ft <sup>2</sup>	Pa.s	$4.778 \times 10^1$

## References

Holman, J.P., “*Heat Transfer 8<sup>th</sup> Edition*”, McGraw-Hill, 6, 293 – 297, 1997.

Jones, T.A., Wooten, S.O. & Kaluza, T.J., “*Single-Phase Flow Through Natural Fractures*”, Society of Petroleum Engineers Annual Technical Conference and Exhibition, Paper Number: 18175-MS, Digital Object Identifier (DOI®): 10.2118/18175-MS, October 2 – 5 1988.

Louis, C., “*A Study of Groundwater in Jointed Rocks and Its Influence on the Stability of Rock Masses*”, Rock Mech. Res., Rep. 10, 90pp, Imp. Coll., London, 1969.

Massachusetts Institute of Technology, “*The Future of Geothermal Energy: Impact of Enhanced Geothermal Systems (EGS) on the United States in the 21<sup>st</sup> Century*”, 4, 5.

McDonald, K.T., “*Radial Viscous Flow Between Two Parallel Annular Plates*”, Joseph Henry Laboratories, Princeton University, Princeton, NJ 08544, June 25 2000.

Munson. B. R., Young, D. F. and Okiishi, T.H., “*Fundamentals of Fluid Mechanics, Fifth Edition*”, Wiley & Sons, 6 & 8, 280 – 282, 320 – 323, 413 – 415, 2006.

Murphy, H.D., Coxon, M. & McEligot, D.M., “*Symmetric Sink Flow Between Parallel Plates*”, Journal of Fluids Engineering, Vol 100, 477 – 484, December 1978.

Patel, V.C., & Head, M.R., “*Reversion of Turbulent to Laminar Flow*”, Journal of Fluid Mechanics, Vol. 43, 371 – 392, 1968.

Slider, H.C., “*Worldwide Practical Petroleum Reservoir Engineering Methods*”, Pennwell Publishing Company, 2, 48 – 49.

Spang, B. “*Thermodynamic and Transport Properties of Water and Steam*”, <http://www.cheresources.com/iapwsif97.shtml#addin>, 2008.

Wyborn, D., de Graaf, L., Davidson, S. & Hann, S., “*Development of Australia’s first hot fractured rock (HFR) underground heat exchanger, Cooper Basin, South Australia*”, In: Boulton, P.J. & Lang, S.C. (Eds), Eastern Australasian Basins Symposium II, Petroleum Exploration Society of Australia, Special Publication, 425.

## Appendix A: Model Derivation

The equations used for the injection and production wells are traditional pipe flow equations and hence do not require derivation here. However if the reader is interested to understand the origins of those equations they are directed to *Fundamentals of Fluid mechanics 5<sup>th</sup> edition* (Munson, Young & Okiishi 2006).

The equations used for fracture flow in this report are derived by the author. The author would like to acknowledge Munson et al 2006 and McDonald 2000 as the primary references for the following derivation.

### Linear Flow

The situation for linear flow is depicted in figure 28. Here the water flows only in the x direction between two parallel plates with the no-slip condition for viscous fluids forming the velocity profile in the y direction.

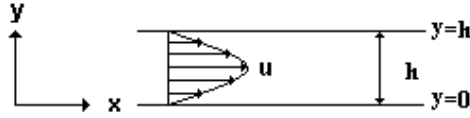


**Figure 28** Viscous linear flow between parallel plates.

For this problem the governing differential equations of motion for incompressible Newtonian fluids, the Navier-Stokes equations, need to be solved. For Cartesian coordinates they are:

$$\rho \left( \frac{\partial u}{\partial t} + u \frac{\partial u}{\partial x} + v \frac{\partial u}{\partial y} + w \frac{\partial u}{\partial z} \right) = -\frac{\partial p}{\partial x} + \rho g_x + \mu \left( \frac{\partial^2 u}{\partial x^2} + \frac{\partial^2 u}{\partial y^2} + \frac{\partial^2 u}{\partial z^2} \right) \quad \text{x direction}$$

$$\rho \left( \frac{\partial v}{\partial t} + u \frac{\partial v}{\partial x} + v \frac{\partial v}{\partial y} + w \frac{\partial v}{\partial z} \right) = -\frac{\partial p}{\partial y} + \rho g_y + \mu \left( \frac{\partial^2 v}{\partial x^2} + \frac{\partial^2 v}{\partial y^2} + \frac{\partial^2 v}{\partial z^2} \right) \quad \text{y direction}$$

$$\rho \left( \frac{\partial w}{\partial t} + u \frac{\partial w}{\partial x} + v \frac{\partial w}{\partial y} + w \frac{\partial w}{\partial z} \right) = -\frac{\partial p}{\partial z} + \rho g_z + \mu \left( \frac{\partial^2 w}{\partial x^2} + \frac{\partial^2 w}{\partial y^2} + \frac{\partial^2 w}{\partial z^2} \right) \quad \text{z direction}$$

Where u is the fluid velocity in the x direction, v is the velocity in the y direction and w is the velocity in the z direction. The continuity equation is:

$$\frac{\partial \rho}{\partial t} + \frac{\partial(\rho u)}{\partial x} + \frac{\partial(\rho v)}{\partial y} + \frac{\partial(\rho w)}{\partial z} = 0$$

Thus assuming constant density and no flow in the y or z directions, the continuity equation becomes:

$$\frac{\partial u}{\partial x} = 0$$

The model is at steady state so therefore  $u$  does not vary with time. Hence the Navier-Stokes equations reduce to:

$$0 = -\frac{\partial p}{\partial x} + \mu \left( \frac{\partial^2 u}{\partial y^2} \right) \quad \text{x direction}$$

$$0 = -\frac{\partial p}{\partial y} + \rho g_y \quad \text{y direction}$$

$$0 = -\frac{\partial p}{\partial z} \quad \text{z direction}$$

It can be seen that the only variation of pressure with respect to gravity is in the  $y$  direction. However the aperture of the fractures is not large enough to significantly alter the pressure drop in this direction. Therefore this term, along with the pressure drop in the  $z$  direction can be ignored, as the latter is constant. Hence the equation of interest is the reduced form of the Navier-Stokes equation in the  $x$  direction, which can be rearranged to the following:

$$\frac{\partial^2 u}{\partial y^2} = \frac{1}{\mu} \frac{\partial p}{\partial x}$$

Integrating twice with respect  $y$  to yields:

$$u = \frac{1}{2\mu} \left( \frac{\partial p}{\partial x} \right) y^2 + c_1 y + c_2$$

Where  $c_1$  and  $c_2$  are constants. Then applying the no-slip boundary conditions (at  $y = 0$  &  $h$ ,  $u = 0$ ):

$$c_2 = 0$$

$$c_1 = -\frac{1}{2\mu} \left( \frac{\partial p}{\partial x} \right) h$$

Therefore the expression for  $u$  becomes:

$$u = \frac{1}{2\mu} \left( \frac{\partial p}{\partial x} \right) y(y-h)$$

Integrating with respect to  $y$  between 0 and  $h$  yields an expression for the volumetric flow rate  $q$  (per unit width in the  $z$  direction):

$$q = \int_0^h \frac{1}{2\mu} \left( \frac{\partial p}{\partial x} \right) y(y-h) \delta y$$

$$q = \frac{1}{2\mu} \left( \frac{\partial p}{\partial x} \right) \int_0^h (y^2 - yh) \delta y$$

$$q = -\frac{1}{2\mu} \left( \frac{\partial p}{\partial x} \right) \frac{h^3}{6}$$

Letting:  $-\frac{\partial p}{\partial x} = \frac{\Delta P}{L'}$  then:

$$q = \frac{\Delta P h^3}{12\mu L'}$$

For fracture width,  $w$ , the expression for flow between parallel plates is:

$$q = \frac{h^3 w \Delta P}{12\mu L'}$$

Thus the cubic law is obtained. Given that the cross sectional area of flow in the linear section is constant, the velocity of the flow is constant and is expressed as:

$$\hat{u} = \frac{q}{A} = \frac{q}{wh}$$

Rearranging for flow rate:

$$q = \hat{u}wh$$

Substituting this expression for flow rate into the cubic law yields:

$$\hat{u}wh = \frac{h^3 w \Delta P}{12\mu L'}$$

$$\hat{u} = \frac{h^2 \Delta P}{12\mu L'}$$

Rearranging for pressure drop:

$$\Delta P = \frac{12\mu \hat{u} L'}{h^2}$$

Expressing pressure drop as a dimensionless quantity by dividing both sides by dynamic pressure  $\frac{1}{2} \rho \hat{u}^2$  yields:

$$\frac{2\Delta P}{\rho \hat{u}^2} = \frac{24\mu \hat{u} L'}{\rho \hat{u}^2 h^2}$$

$$\frac{2\Delta P}{\rho \hat{u}^2} = \frac{48}{\text{Re}} \frac{L'}{h}$$

$$\Delta P = \frac{24}{\text{Re}} \rho \frac{L'}{h} \hat{u}^2$$

Thus the equation for pressure drop for radial flow between 2 smooth parallel plates is obtained, where Re is the Reynolds number for flow through a fracture, which is:

$$\text{Re} = \frac{2h\rho\hat{u}}{\mu}$$

In pipe flow, the friction factor,  $f$ , for laminar flow would be given by:

$$f = \frac{24}{\text{Re}}$$

To account for roughness of rock surfaces, the empirically governed relation developed by Louis (1969) is modified to form the friction factor for laminar fracture flow:

$$f_f = \left( \frac{24}{\text{Re}} \right) \left( 1 + 3.1 \left( \frac{\varepsilon}{h} \right)^{1.5} \right)$$

Thus the final expression for linear flow pressure drop is:

$$\Delta P_{lin} = f_f \rho \frac{L'}{h} \hat{u}^2$$

## Radial Flow

The situation for deriving the radial flow equation is shown below in figure 29:

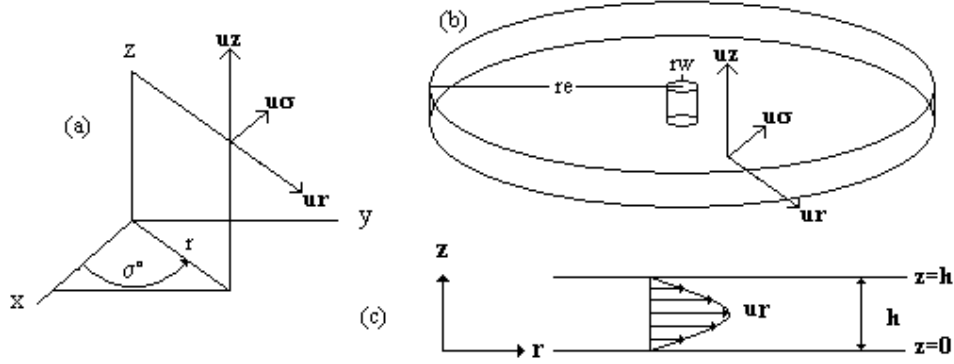


**Figure 29** (a) Cylindrical coordinate system (b) velocity vectors at any point between two parallel discs (c) velocity profile in z direction due to no-slip condition.

Figure 29 (a) shows how cylindrical coordinates relate to regular Cartesian coordinates, (b) shows how the velocity vectors for each cylindrical direction are orientated at any point within two parallel discs and (c) shows the variation of  $u_r$  with respect to  $z$ . The Navier-Stokes and continuity equations for this arrangement are:

(r direction)

$$\begin{aligned} \rho \left( \frac{\partial u_r}{\partial t} + u_r \frac{\partial u_r}{\partial r} + \frac{u_\sigma}{r} \frac{\partial u_r}{\partial \sigma} - \frac{u_\sigma^2}{r} + u_z \frac{\partial u_r}{\partial z} \right) \\ = -\frac{\partial p}{\partial r} + \rho g_r + \mu \left[ \frac{1}{r} \frac{\partial}{\partial r} \left( r \frac{\partial u_r}{\partial r} \right) - \frac{u_r}{r^2} + \frac{1}{r^2} \frac{\partial^2 u_r}{\partial \sigma^2} - \frac{2}{r^2} \frac{\partial u_\theta}{\partial \sigma} + \frac{\partial^2 u_r}{\partial z^2} \right] \end{aligned}$$

( $\sigma$  direction)

$$\begin{aligned} \rho \left( \frac{\partial u_\sigma}{\partial t} + u_r \frac{\partial u_\sigma}{\partial r} + \frac{u_\sigma}{r} \frac{\partial u_\sigma}{\partial \sigma} - \frac{u_r u_\sigma}{r} + u_z \frac{\partial u_\sigma}{\partial z} \right) \\ = -\frac{1}{r} \frac{\partial p}{\partial \sigma} + \rho g_\sigma + \mu \left[ \frac{1}{r} \frac{\partial}{\partial r} \left( r \frac{\partial u_\sigma}{\partial r} \right) - \frac{u_\sigma}{r^2} + \frac{1}{r^2} \frac{\partial^2 u_\sigma}{\partial \sigma^2} - \frac{2}{r^2} \frac{\partial u_r}{\partial \sigma} + \frac{\partial^2 u_\sigma}{\partial z^2} \right] \end{aligned}$$

(z direction)

$$\begin{aligned} \rho \left( \frac{\partial u_z}{\partial t} + u_r \frac{\partial u_z}{\partial r} + \frac{u_\sigma}{r} \frac{\partial u_z}{\partial \sigma} + u_z \frac{\partial u_z}{\partial z} \right) \\ = -\frac{\partial p}{\partial z} + \rho g_z + \mu \left[ \frac{1}{r} \frac{\partial}{\partial r} \left( r \frac{\partial u_z}{\partial r} \right) + \frac{1}{r^2} \frac{\partial^2 u_z}{\partial \sigma^2} + \frac{\partial^2 u_z}{\partial z^2} \right] \end{aligned}$$

Continuity:

$$\frac{1}{r} \frac{\partial}{\partial r} (ru_r) + \frac{1}{r} \frac{\partial u_\sigma}{\partial \sigma} + \frac{\partial u_z}{\partial z} = 0$$

Assuming that flow is in the radial direction only (that is  $u_z = u_\sigma = 0$ ) and that it is steady (that is  $u_r$  does not vary with time or in the  $\sigma$  direction) the cylindrical Navier-Stokes equations reduce to:

$$\rho u_r \frac{\partial u_r}{\partial r} = - \frac{\partial p}{\partial r} + \mu \frac{\partial^2 u_r}{\partial z^2} \quad (\text{r direction})$$

$$0 = - \frac{1}{r} \frac{\partial p}{\partial \sigma} \quad (\text{\sigma direction})$$

$$0 = \frac{\partial p}{\partial z} + \rho g_z \quad (\text{z direction})$$

It can be seen from the reduced equations that pressure varies only in the z and r direction. However, given the aperture of a fracture is so small, pressure does not vary significantly in the z direction. Therefore the z direction equation can be ignored. The pressure gradient in the  $\sigma$  direction is constant hence that equation can also be ignored. The continuity equation, for the given conditions, can be reduced to:

$$\frac{1}{r} \frac{\partial}{\partial r} (ru_r) = 0 \quad (*)$$

It can be seen from figure 29 (c) that  $u_r$  is a function of z. velocity is also a function of r as the cross-sectional area of flow changes with respect to radius. Using equation (\*) to derive an expression for  $u_r$ :

$$\frac{1}{r} \frac{\partial}{\partial r} (ru_r) = 0$$

$$\frac{\partial}{\partial r} (ru_r) = 0$$

Then integrating with respect to r:

$$\int \frac{\partial}{\partial r} (ru_r) \partial r = \int 0 \partial r$$

$$ru_r = F(z)$$

$$u_r(r,z) = \frac{F(z)}{r} \quad (**)$$

Thus an expression is obtained for  $u_r(r, z)$  with the  $r$  dependency already defined, all that now needs to be determined is the function  $F(z)$ . Substituting equation \*\* into the reduced  $r$  direction equation yields:

$$\mu \frac{\partial^2}{\partial z^2} \left( \frac{F(z)}{r} \right) = \frac{\partial p}{\partial r} + \frac{\rho F(z)}{r} \frac{\partial}{\partial r} \left( \frac{F(z)}{r} \right)$$

$$\mu \frac{\partial}{\partial z} \left( \frac{1}{r} \frac{\partial F(z)}{\partial z} \right) = \frac{\partial p}{\partial r} + \frac{\rho F(z)}{r} \left( -\frac{F(z)}{r^2} \right)$$

$$\frac{\mu}{r} \frac{\partial^2 F}{\partial z^2} = \frac{\partial p}{\partial r} - \frac{\rho}{r^3} F^2$$

$$r^3 \frac{\partial p}{\partial r} = \mu r^2 \frac{\partial^2 F}{\partial z^2} + \rho F^2$$

In attempting to obtain an approximate solution to this flow regime, the non-linear term  $F^2$  should be ignored (McDonald 2000). The expression then becomes:

$$r^3 \frac{\partial p}{\partial r} = \mu r^2 \frac{\partial^2 F}{\partial z^2}$$

$$\frac{\partial^2 F}{\partial z^2} = \frac{r}{\mu} \frac{\partial p}{\partial r}$$

Now integrating with respect to  $z$  and thus treating  $\frac{\partial p}{\partial r}$  as a constant

$$\int \frac{\partial^2 F}{\partial z^2} \partial z = \int \frac{r}{\mu} \frac{\partial p}{\partial r} \partial z$$

$$\frac{\partial F}{\partial z} = \frac{r}{\mu} \frac{\partial p}{\partial r} z + c_1$$

Where  $c_1$  is a constant. Again integrating with respect to  $z$  to determine an expression for  $F$ :

$$\int \frac{\partial F}{\partial z} \partial z = \int \left( \frac{r}{\mu} \frac{\partial p}{\partial r} z + c_1 \right) \partial z$$

$$F = \frac{r}{2\mu} \frac{\partial p}{\partial r} z^2 + c_1 z + c_2$$

Now applying the boundary conditions of  $u_r = F = 0$  at  $z = 0, h$ .

$$0 = 0^2 \times \frac{r}{2\mu} \frac{\partial p}{\partial r} + 0 \times c_1 + c_2$$

$$c_2 = 0$$

$$0 = h^2 \times \frac{r}{2\mu} \frac{\partial p}{\partial r} + h \times c_1$$

$$c_1 = -\frac{r}{2\mu} \frac{\partial p}{\partial r} h$$

Therefore the expression for the function F is:

$$F = \frac{r}{2\mu} \frac{\partial p}{\partial r} z^2 - \frac{r}{2\mu} \frac{\partial p}{\partial r} hz$$

$$F = \frac{r}{2\mu} \frac{\partial p}{\partial r} z(z-h)$$

Now rearranging and separating the variables, then integrating between  $r_w$  and  $r_e$  with respect to  $r$  and between  $p_w$  and  $p_e$  with respect to  $p$ :

$$\frac{2\mu F}{z(z-h)} \frac{1}{r} \partial r = \partial p$$

$$\frac{2\mu F}{z(z-h)} \int_{r_w}^{r_e} \frac{\partial r}{r} = \int_{p_w}^{p_e} \partial p$$

$$\frac{2\mu F}{z(z-h)} \ln r \Big|_{r_w}^{r_e} = p \Big|_{p_w}^{p_e}$$

$$\frac{2\mu F}{z(z-h)} (\ln r_e - \ln r_w) = p_e - p_w$$

$$\frac{2\mu F \ln \left( \frac{r_e}{r_w} \right)}{z(z-h)} = -\Delta P$$

Now substituting in the expression for F:

$$F = u_r r$$

$$2\mu u_r r \ln\left(\frac{r_e}{r_w}\right) = \Delta P z (h - z)$$

$$u_r = \frac{\Delta P z (h - z)}{2\mu r \ln\left(\frac{r_e}{r_w}\right)}$$

This equation is the expression of  $u_r$  as a function of  $r$  and  $z$ . The volumetric flow rate passing between the plates can be determined (for unit circumference) by integrating between  $h$  and  $0$  with respect to  $z$ .

$$q = \int_0^h v_r \partial z = \frac{\Delta P}{2\mu r \ln\left(\frac{r_e}{r_w}\right)} \int_0^h z (h - z) \partial z$$

$$q = \frac{\Delta P}{2\mu r \ln\left(\frac{r_e}{r_w}\right)} \int_0^h (zh - z^2) \partial z$$

$$q = \frac{\Delta P}{2\mu r \ln\left(\frac{r_e}{r_w}\right)} \left[ \frac{z^2 h}{2} - \frac{z^3}{3} \right]_0^h$$

$$q = \frac{\Delta P}{2\mu r \ln\left(\frac{r_e}{r_w}\right)} \left( \frac{h^3}{2} - \frac{h^3}{3} \right)$$

$$q = \frac{h^3 \Delta P}{12\mu r \ln\left(\frac{r_e}{r_w}\right)}$$

Multiplying by the circumference with radius r:

$$q = \frac{h^3 \Delta P}{12 \mu r \ln\left(\frac{r_e}{r_w}\right)} \times 2\pi r$$

$$q = \frac{h^3 \pi \Delta P}{6 \mu \ln\left(\frac{r_e}{r_w}\right)}$$

Thus the approximate cubic law for radial flow between parallel discs is obtained. The flow in the radial section is modified to accommodate for an angle  $\theta$  at which the no flow boundaries are positioned:

$$\frac{q}{\left(\frac{\theta}{360}\right)} = \frac{h^3 \pi \Delta P}{6 \mu \ln\left(\frac{r_e}{r_w}\right)}$$

The velocity of water at radius r is therefore:

$$u_r = \frac{q}{\frac{\theta}{360} 2\pi r h}$$

$$u_r = \frac{180q}{\theta \pi r h}$$

The average velocity between  $r_e$  and  $r_w$  is therefore:

$$\hat{u} = \frac{1}{r_e - r_w} \int_{r_w}^{r_e} v \partial r$$

$$\hat{u} = \frac{1}{r_e - r_w} \frac{180q}{\theta \pi h} \int_{r_w}^{r_e} \frac{1}{r} \partial r$$

$$\hat{u} = \frac{180q \ln\left(\frac{r_e}{r_w}\right)}{(r_e - r_w) \theta \pi h}$$

Rearranging for flow rate:

$$q = \frac{\hat{u}(r_e - r_w)\theta\pi h}{180 \ln\left(\frac{r_e}{r_w}\right)}$$

Substituting this into the approximate cubic law and rearranging for pressure drop:

$$\frac{\hat{u}(r_e - r_w)\theta\pi h}{180 \ln\left(\frac{r_e}{r_w}\right)} \frac{360}{\theta} = \frac{h^3 \pi \Delta P}{6 \mu \ln\left(\frac{r_e}{r_w}\right)}$$

$$\hat{u} = \frac{h^2 \Delta P}{12 \mu (r_e - r_w)}$$

$$\Delta P = \frac{12 \hat{u} \mu (r_e - r_w)}{h^2}$$

Expressing pressure drop as a dimensionless quantity by dividing both sides by dynamic pressure (valid for any streamline) yields:

$$\frac{2 \Delta P}{\rho \hat{u}^2} = \frac{24 \hat{u} \mu (r_e - r_w)}{\rho \hat{u}^2 h^2}$$

$$\frac{2 \Delta P}{\rho \hat{u}^2} = \frac{48}{\text{Re}} \frac{(r_e - r_w)}{h}$$

$$\Delta P = \frac{24}{\text{Re}} \rho \frac{(r_e - r_w)}{h} \hat{u}^2$$

To account for rock relative roughness the modified Louis (1969) friction factor is again used. Thus the final expression for laminar radial flow pressure drop is:

$$\Delta P_{rad} = f_f \rho \frac{r_e - r_w}{h} \hat{u}_{rad}^2$$

### Overall Reynolds Number

Murphy et al defined overall Reynolds as  $\text{Re}_o = \frac{q}{4 \pi \nu t}$ , where q is volumetric flow rate,  $\nu$  is kinematic viscosity and t is half the distance between the parallel discs. In this study  $t = \frac{h}{2}$  and

$\nu = \frac{\mu}{\rho}$  so  $\text{Re}_o$  becomes:

$$Re_o = \frac{q\rho}{2\pi\mu h}$$

This would be overall Reynolds for 360° radial flow. However in this study, one of the variables is the angle of radial flow subtended by the geometry of the fractures. Therefore overall Reynolds becomes:

$$Re_o = \frac{180q_{pf}\rho}{\pi\theta\mu h}$$

### Assumption Validation

An important assumption of the model was that the water is heated up to reservoir temperature almost instantly as soon as it enters the fractures. To show that this assumption is valid the following short heat transfer calculation is presented:

Problem:

For a fracture of width 200m and aperture 0.5mm, what length of flow is required to heat water flowing at 10kg/s initially at 98°C to the reservoir temperature of 250°C? The average pressure in the reservoir is 10000psia.

Solution:

Assume that both sides of the fracture are at constant temperature. Therefore the Nusselt number for constant temperature parallel plates is 7.541 (Holman 1997).

$$Nu_T = 7.541$$

The inlet bulk temperature is 98°C and the ultimate bulk temperature is 250°C. Therefore at an average bulk temperature of 174°C and reservoir temperature 10000psia the properties of water are:

$$\begin{aligned}\rho_{avg} &= 931.4 \text{ kg.m}^{-3}, \quad \mu_{avg} = 1.171 \times 10^{-4} \text{ Pa.s}, \\ k_{avg} &= 0.7246 \text{ W.m}^{-1} \text{ K}^{-1}, \quad c_p = 4173 \text{ J.kg}^{-1} \text{ K}^{-1}\end{aligned}$$

Therefore calculating the heat transfer coefficient:

$$\hat{h} = \frac{Nu_T k_{avg}}{2h} = \frac{7.541 \times 0.724 \text{ W.m}^{-1} \text{ K}^{-1}}{2 \times 0.0005 \text{ m}} = 5460 \text{ W.m}^{-2} \text{ K}^{-1}$$

The two heat flow equations for this scenario are:

$Q = c_p m (T_{b2} - T_{b1})$  and  $Q = \hat{h} A (T_w - T_{bavg})$  where A is the area of the flow and is equal to  $A = 2(w + h)L$ .

Therefore equating these two expressions and solving for length L:

$$c_p m (T_{b2} - T_{b1}) = 2\hat{h}(w + h)L(T_w - T_{bavg})$$

$$L = \frac{c_p m (T_{b2} - T_{b1})}{2\hat{h}(w + h)(T_w - T_{bavg})}$$

$$L = \frac{4173 J \cdot kg^{-1} \cdot K^{-1} \times 10 kg \cdot s^{-1} \times (250 - 98) K}{2 \times 5460 J \cdot s^{-1} \cdot m^{-2} \cdot K^{-1} \times (200 + 0.0005) m (250 - 174) K}$$

$$L = 0.0382 m$$

So in just over a foot of flow length, the water has already heated up to 250°C. This is a result of the wide heat transfer associated with flow between parallel plates.

## Appendix B: Sample Calculation

The following example demonstrates the workings of the model:

A hydraulically fractured geothermal reservoir consists of 20 fractures with a rock temperature of 250°C and pressure of 10000psia. Each fracture is identical with aperture 0.5mm and width 250m. The angle of radial flow is 90° and the roughness of the rock is 0.25mm. One injection well and one production well are drilled to the fracture zone at a depth of 4500m. Both are cased with commercial steel. The wells are 8 inches in diameter and 750m apart. The reinjection temperature is 98°C and water is being produced at 240°C. For a mass flow rate of 100kg/s determine:

- the reservoir pressure drop;
- the required injection pressure; and
- the resulting injection pressure

### Solution:

The problem variables are summarised below in table II:

**Table II** Problem variables summarised.

Variable	Symbol	Value	Units
Mass flow rate	m	100	kg/s
Reservoir depth	D	4500	m
Reservoir temperature	T <sub>r</sub>	250	°C
Reservoir pressure	P <sub>r</sub>	10000	psia
Fracture aperture	h	0.5	mm
Fracture width	w	250	m
Number of fractures	n	20	-
Distance between wells	L	750	m
Reinjection temperature	T <sub>i</sub>	98	°C
Production Temperature	T <sub>p</sub>	240	°C
Angle of radial flow	θ	90	°
Rock roughness	ε	0.25	mm
Well diameter	d <sub>w</sub>	8	in

- Reservoir pressure drop

First determine external radius and length of linear flow section:

$$r_e = \frac{w}{2 \sin\left(\frac{\theta}{2}\right)} = \frac{250m}{2 \sin 45^\circ} = 176.8m$$

$$L' = L - 2r_e = 750m - 2 \times 176.8m = 396.4m$$

Second determine the properties of water at reservoir conditions:

$$T_r = 250^\circ C = 250 + 273.15K = 523.15K$$

$$P_r = 10000 \text{ psia} = \frac{10000}{14.5037738} \text{ bar} = 689.48 \text{ bar}$$

Then using Microsoft Excel® Add-in *Water97\_v13.xla* (version 1.3), syntax in cell A1:

$$= \text{densW}(523.15, 689.48) = 856.5 \text{ kg.m}^{-3}$$

In cell A2:

$$= \text{viscW}(523.15, 689.48) = 1.214 \times 10^{-4} \text{ Pa.s}$$

$$\therefore \rho_r = 856.5 \text{ kg.m}^{-3} \text{ and } \mu_r = 1.214 \times 10^{-4} \text{ Pa.s}$$

Now calculate linear flow section

Velocity:

$$\hat{u} = \frac{q_{pf}}{A}$$

$$\hat{u} = \frac{m}{n\rho A} = \frac{m}{n\rho wh}$$

$$\hat{u} = \frac{100 \text{ kg.s}^{-1}}{20 \times 856.5 \text{ kg.m}^{-3} \times 250 \text{ m} \times 0.0005 \text{ m}} = 0.0467 \text{ m.s}^{-1}$$

Reynolds number:

$$\text{Re}_f = \frac{2h\rho_r\hat{u}}{\mu_r}$$

$$\text{Re}_f = \frac{2 \times 0.0005 \text{ m} \times 856.5 \text{ kg.m}^{-3} \times 0.0467 \text{ m.s}^{-1}}{1.214 \times 10^{-4} \text{ kg.m}^{-1} \text{ .s}^{-1}} = 329.47$$

$\therefore \text{Re} < 2300$  so flow is laminar and linear flow solution will be valid.

Friction factor:

$$f_f = \left( \frac{24}{\text{Re}} \right) \left( 1 + 3.1 \left( \frac{\varepsilon}{h} \right)^{1.5} \right)$$

$$f_f = \frac{24}{329.47} \left( 1 + 3.1(0.5)^{1.5} \right) = 0.153$$

Pressure Drop:

$$\Delta P_{lin} = f_f \rho_r \frac{L'}{h} \hat{u}^2$$

$$\Delta P_{lin} = 0.153 \times 856.5 \text{ kg.m}^{-3} \times \frac{396.4 \text{ m}}{0.0005 \text{ m}} \times (0.0467 \text{ m.s}^{-1})^2$$

$$\Delta P_{lin} = 226600 \text{ Pa} = 32.86 \text{ psia}$$

Now calculate radial sections

Velocity:

$$\hat{u}_{rad} = \frac{180 q_{pf} \ln\left(\frac{r_e}{r_w}\right)}{(r_e - r_w) \theta \pi h}$$

$$\hat{u}_{rad} = \frac{180 \times \frac{100 \text{ kg.s}^{-1}}{20 \times 856.5 \text{ kg.m}^{-3}} \ln\left(\frac{176.8 \text{ m}}{\frac{8 \times 0.0254 \text{ m}}{2}}\right)}{\left(176.8 \text{ m} - \frac{8 \times 0.0254 \text{ m}}{2}\right) \times 90 \times 3.14 \times 0.0005 \text{ m}} = 0.314 \text{ m.s}^{-1}$$

Reynolds number:

$$\text{Re}_f = \frac{2 \times 0.0005 \text{ m} \times 856.5 \text{ kg.m}^{-3} \times 0.314 \text{ m.s}^{-1}}{1.214 \times 10^{-4} \text{ kg.m}^{-1} \text{.s}^{-1}} = 2214$$

Overall Reynolds number (validity check):

$$\text{Re}_o = \frac{180 q_{pf} \rho}{\pi \theta \mu h}$$

$$\text{Re}_o = \frac{180 \times \frac{100 \text{ kg.s}^{-1}}{20 \times 856.5 \text{ kg.m}^{-3}} \times 856.5 \text{ kg.m}^{-3}}{3.14 \times 90 \times 1.214 \times 10^{-4} \text{ kg.m}^{-1} \text{.s}^{-1} \times 0.0005 \text{ m}} = 5.24 \times 10^7$$

$\therefore \text{Re}_o < 1 \times 10^8$  so radial solution is also valid.

Friction factor:

$$f_f = \frac{24}{2214} \left(1 + 3.1 \times (0.5)^{1.5}\right) = 0.0227$$

Pressure Drop:

$$\Delta P_{rad} = 0.0227 \times 856.5 \text{ kg.m}^{-3} \times \frac{\left(176.8 \text{ m} - \frac{8 \times 0.0254 \text{ m}}{2}\right)}{0.0005 \text{ m}} \times (0.314 \text{ m.s}^{-1})^2$$

$$\Delta P_{rad} = 677400 \text{ Pa} = 98.26 \text{ psia}$$

Total reservoir pressure drop is therefore:

$$\begin{aligned}\Delta P_r &= \Delta P_{lin} + 2\Delta P_{rad} \\ \Delta P_r &= 32.86 \text{ psia} + 2 \times 98.26 \text{ psia} = 229.4 \text{ psia}\end{aligned}$$

Total reservoir pressure drop is therefore 229.4psia.

(b) Required injection pressure

First the average properties of water need to be determined. However to do this the required injection must be known. Therefore  $P_i$  must be guessed.

Guess:

$$P_{i0} = 4000 \text{ psia}$$

Injection wellbore pressure:

$$P_{iw} = P_r + \frac{\Delta P_r}{2} = 10000 \text{ psia} + \frac{229.4}{2} \text{ psia} = 10114.7 \text{ psia}$$

Average pressure is therefore:

$$P_{iavg} = \frac{4000 \text{ psia} + 10114.7 \text{ psia}}{2} = 7057.35 \text{ psia}$$

Again using Excel®:

$$\rho_i = \text{densW}\left(98 + 273.15, \frac{7057.35}{14.5037738}\right) = 981.0 \text{ kg.m}^{-3}$$

And

$$\mu_i = \text{viscW}\left(98 + 273.15, \frac{7057.35}{14.5037738}\right) = 3.000 \times 10^{-4} \text{ Pa.s}$$

Velocity:

$$\hat{u} = \frac{m}{\rho_i A}$$

$$\hat{u} = \frac{m}{\rho_i \pi \left(\frac{d_w}{2}\right)^2}$$

$$\hat{u} = \frac{100 \text{ kg.s}^{-1}}{981.0 \text{ kg.m}^{-3} \times 3.14 \times \left(\frac{8 \times 0.0254 \text{ m}}{2}\right)^2} = 3.143 \text{ m.s}^{-1}$$

Reynolds number:

$$\text{Re}_i = \frac{d_w \rho_i \hat{u}}{\mu_i}$$

$$\text{Re}_i = \frac{8 \times 0.0254 \text{ m} \times 981.0 \text{ kg.m}^{-3} \times 3.143 \text{ m.s}^{-1}}{3.00 \times 10^{-4} \text{ kg.m}^{-1} \text{ .s}^{-1}} = 1043208$$

$Re_i > 2300$  so flow is turbulent

From Moody's roughness chart for commercial pipes:

$$\frac{\varepsilon}{d_w} = 0.000225$$

Friction factor (initial guess from Blasius equation):

$$f = 0.3164 Re_i^{-0.25}$$

$$f = 0.3164 \times 1043208^{-0.25} = 9.900 \times 10^{-3}$$

Now using the Colebrook equation and iterating:

$$f_1 = \frac{0.25}{\left\{ \log \left[ \frac{\varepsilon/d_w}{3.7} + \frac{2.51}{(Re_i \sqrt{f_0})} \right] \right\}^2}$$

$$f_1 = \frac{0.25}{\left\{ \log \left[ \frac{0.000225}{3.7} + \frac{2.51}{(1043208 \times \sqrt{9.900 \times 10^{-3}})} \right] \right\}^2} = 0.0150876$$

$$f_2 = \frac{0.25}{\left\{ \log \left[ \frac{0.000225}{3.7} + \frac{2.51}{(1043208 \times \sqrt{0.0150876})} \right] \right\}^2} = 0.0141598$$

$$f_3 = \frac{0.25}{\left\{ \log \left[ \frac{0.000225}{3.7} + \frac{2.51}{(1043208 \times \sqrt{0.0141598})} \right] \right\}^2} = 0.0141627$$

$$f_4 = \frac{0.25}{\left\{ \log \left[ \frac{0.000225}{3.7} + \frac{2.51}{(1043208 \times \sqrt{0.0141627})} \right] \right\}^2} = 0.0141627$$

Therefore  $f_i = 0.0141627$

Pressure drop:

$$\Delta P_i = f_i \rho_i \frac{D}{d_w} \frac{\hat{u}^2}{2} - \rho_i g (z_1 - z_2)$$

$$\Delta P_i = 0.0141627 \times 981.0 \text{ kg.m}^{-3} \times \frac{4500}{8 \times 0.0254} \times \frac{(3.14 \text{ m.s}^{-1})^2}{2} - 981.0 \text{ kg.m}^{-3} \times 9.81 \text{ m.s}^{-2} (0 \text{ m} - (-4500 \text{ m}))$$

$$\Delta P_i = -41789000 \text{ Pa} = -6061 \text{ psia}$$

Required injection pressure:

$$\begin{aligned}\Delta P_i &= P_i - P_{iw} \\ P_i &= P_{wi} + \Delta P_i = 10114.7 \text{ psia} - 6061 \text{ psia} \\ P_i &= 4053.7 \text{ psia}\end{aligned}$$

The initial guess was 4000psia. Therefore this new value needs to be substituted back into the water properties calculations, and the procedure repeated. Eventually required injection pressure converges to an answer of:

$$P_i = 4059 \text{ psia}$$

(c) Resulting production pressure

The calculation process for production pressure is determined in the same manner as injection pressure. An initial guess for production pressure must be made:

Guess:

$$P_{p0} = 4000 \text{ psia}$$

Production wellbore pressure:

$$P_{pw} = P_r - \frac{\Delta P_r}{2} = 10000 \text{ psia} - \frac{229.4}{2} \text{ psia} = 9885.3 \text{ psia}$$

Average pressure is therefore:

$$P_{pavg} = \frac{4000 \text{ psia} + 9885.3 \text{ psia}}{2} = 6942.65 \text{ psia}$$

Again using Excel®:

$$\rho_p = \text{densW}\left(240 + 273.15, \frac{6942.65}{14.5037738}\right) = 852.5 \text{ kg.m}^{-3}$$

And

$$\mu_p = \text{viscW}\left(240 + 273.15, \frac{6942.65}{14.5037738}\right) = 1.216 \times 10^{-4} \text{ Pa.s}$$

Velocity:

$$\hat{u} = \frac{m}{\rho_p A}$$

$$\hat{u} = \frac{m}{\rho_p \pi \left(\frac{d_w}{2}\right)^2}$$

$$\hat{u} = \frac{100 \text{ kg.s}^{-1}}{852.5 \text{ kg.m}^{-3} \times 3.14 \times \left(\frac{8 \times 0.0254 \text{ m}}{2}\right)^2} = 3.617 \text{ m.s}^{-1}$$

Reynolds number:

$$\text{Re}_p = \frac{d_w \rho_p \hat{u}}{\mu_p}$$

$$\text{Re}_p = \frac{8 \times 0.0254 \text{m} \times 852.5 \text{kg.m}^{-3} \times 3.617 \text{m.s}^{-1}}{1.216 \times 10^{-4} \text{kg.m}^{-1}.\text{s}^{-1}} = 2782263$$

$\text{Re}_p > 2300$  so flow is turbulent

From Moody's roughness chart for commercial pipes:

$$\frac{\varepsilon}{d_w} = 0.000225$$

Friction factor (initial guess from Blasius equation):

$$f = 0.3164 \text{Re}_p^{-0.25}$$

$$f = 0.3164 \times 2782263^{-0.25} = 7.747 \times 10^{-3}$$

Now using the Colebrook equation and iterating:

$$f_1 = \frac{0.25}{\left\{ \log \left[ \frac{\varepsilon/d_w}{3.7} + \frac{2.51}{\text{Re}_p \sqrt{f_0}} \right] \right\}^2}$$

$$f_1 = \frac{0.25}{\left\{ \log \left[ \frac{0.000225}{3.7} + \frac{2.51}{1043208 \times \sqrt{7.747 \times 10^{-3}}} \right] \right\}^2} = 0.0152056$$

$$f_2 = \frac{0.25}{\left\{ \log \left[ \frac{0.000225}{3.7} + \frac{2.51}{1043208 \times \sqrt{0.0152056}} \right] \right\}^2} = 0.0149072$$

$$f_3 = \frac{0.25}{\left\{ \log \left[ \frac{0.000225}{3.7} + \frac{2.51}{1043208 \times \sqrt{0.0149072}} \right] \right\}^2} = 0.0149149$$

$$f_4 = \frac{0.25}{\left\{ \log \left[ \frac{0.000225}{3.7} + \frac{2.51}{1043208 \times \sqrt{0.0149149}} \right] \right\}^2} = 0.0149147$$

$$f_5 = \frac{0.25}{\left\{ \log \left[ \frac{0.000225}{3.7} + \frac{2.51}{1043208 \times \sqrt{0.0149147}} \right] \right\}^2} = 0.0149147$$

Therefore  $f_p = 0.0149147$

Pressure drop:

$$\Delta P_p = f_p \rho_p \frac{D}{d_w} \frac{\hat{u}^2}{2} - \rho_p g (z_1 - z_2)$$

$$\Delta P_p = 0.0149147 \times 852.5 \text{ kg.m}^{-3} \times \frac{4500}{8 \times 0.0254} \times \frac{(3.617 \text{ m.s}^{-1})^2}{2} - 852.5 \text{ kg.m}^{-3} \times 9.81 \text{ m.s}^{-2} (-4500 \text{ m} - 0 \text{ m})$$

$$\Delta P_p = 39475506 \text{ Pa} = 5725 \text{ psia}$$

Resulting production pressure:

$$\Delta P_p = P_{pw} - P_p$$

$$P_p = P_{pw} - \Delta P_p = 9885.3 \text{ psia} - 5725 \text{ psia}$$

$$P_p = 4160 \text{ psia}$$

The initial guess was 4000psia. Therefore this new value needs to be substituted back into the water properties calculations, and the procedure repeated. Eventually resulting production pressure converges to an answer of:

$$P_p = 4169 \text{ psia}$$

## Appendix C: Sensitivity Analysis Data

Mass flow rate

**Table III** Inputs for mass flow rate analysis.

Inputs	Symbol	Value	Units
Fracture Aperture	h	0.5	mm
Fracture Breadth	w	200	m
Distance between wells	L	1000	m
Number of fractures	n	10	-
Angle for Radial Flow	$\theta$	90	°
Reservoir Temperature	$T_r$	250	°C
Rock Relative Roughness	$\varepsilon/h$	0.5	m
Reservoir Overburden	$P_r$	10000	psia
Injection Pressure Drop	$\Delta P_i$	-6057	psia
Production Pressure Drop	$\Delta P_p$	5715	psia

**Table IV** Reservoir calculated data.

Reservoir Calculated Data	Symbol	Value	Units
External Radius	$r_e$	141.4213562	m
Linear Section Length	$L'$	717.1572875	m
well radius	$r_w$	0.1016	m
Water Density	$\rho$	856.464211	kg/m <sup>3</sup>
Water Viscosity	$\mu$	1.2143E-04	kg.m.s
Fracture Aperture	h	5.0000E-04	m

**Table V** Linear Section for mass flow rate analysis.

Mass flow rate kg/s	Fluid velocity m/s	Reynolds Number	Friction Factor	Pressure Drop psia	Pressure Gradient psia/m
50	5.8380E-02	411.77	0.122166338	82.8	0.103
60	7.0055E-02	494.12	0.101805281	99.3	0.124
70	8.1731E-02	576.48	0.08726167	115.9	0.145
80	9.3407E-02	658.83	0.076353961	132.4	0.166
90	1.0508E-01	741.19	0.067870188	149.0	0.186
100	1.1676E-01	823.54	0.061083169	165.5	0.207
110	1.2844E-01	905.89	0.055530153	182.1	0.228
120	1.4011E-01	988.25	0.050902641	198.6	0.248

**Table VI** Radial section for mass flow rate analysis.

Mass flow rate kg/s	Average Velocity m/s	Reynolds Number	Overall Reynolds	Friction Factor	Pressure Drop psia	Pressure Gradient psia/m
50	0.2564	1808.48	2.62E+07	0.027815837	45.4	0.454310502
60	0.3077	2170.18	3.15E+07	0.023179864	54.5	0.545172602
70	0.3590	2531.87	3.67E+07	0.019868455	63.5	0.636034703
80	0.4102	2893.57	4.19E+07	0.017384898	72.6	0.726896803
90	0.4615	3255.26	4.72E+07	0.015453243	81.7	0.817758903
100	0.5128	3616.96	5.24E+07	0.013907919	90.8	0.908621004
110	0.5641	3978.65	5.77E+07	0.012643562	99.8	0.999483104
120	0.6154	4340.35	6.29E+07	0.011589932	108.9	1.090345204

**Table VII** Mass flow rate analysis results.

Injection pressure psia	Production pressure psia	Total reservoir $\Delta P$ psia	Bottom hole injection pressure psia	Pressure at injection external radius psia	Pressure at production external radius psia	Bottom hole production pressure psia
4029.8	4198.6	173.52	10086.8	10041.4	9958.6	9913.2
4047.2	4181.3	208.23	10104.1	10049.7	9950.3	9895.9
4064.5	4163.9	242.93	10121.5	10057.9	9942.1	9878.5
4081.9	4146.6	277.64	10138.8	10066.2	9933.8	9861.2
4099.2	4129.2	312.34	10156.2	10074.5	9925.5	9843.8
4116.6	4111.9	347.05	10173.5	10082.8	9917.2	9826.5
4133.9	4094.5	381.75	10190.9	10091.0	9909.0	9809.1
4151.3	4077.2	416.45	10208.2	10099.3	9900.7	9791.8
		Distance along reservoir	0	100	900	1000

## Fracture Aperture

**Table VIII** Inputs for fracture aperture analysis.

Inputs	Symbol	Value	Units
Mass flow rate	m	100	kg/s
Fracture breadth	w	200	m
Distance between wells	L	1000	m
Number of fractures	n	10	-
Angle for radial flow	$\theta$	180	°
Reservoir temperature	$T_r$	250	°C
Rock relative roughness	$\varepsilon/h$	0.5	m
Reservoir pressure	$P_r$	10000	psia
Injection pressure drop	$\Delta P_i$	-6057	psia
Production pressure drop	$\Delta P_p$	5715	psia

**Table IX** Reservoir calculated data for fracture aperture analysis.

Reservoir Calculated Data	Symbol	Value	Unit
External Radius	$r_e$	100	m
Linear Section Length	$L'$	800	m
Well radius	$r_w$	0.1016	m
Water density	R	856.464211	kg/m <sup>3</sup>
Water viscosity	$\mu$	1.2143E-04	kg.m.s

**Table X** Linear section for fracture aperture analysis.

Fracture Aperture mm	Fluid Velocity m/s	Reynolds Number	Friction Factor	Pressure Drop psia	Pressure Gradient psia/m
0.25	2.3352E-01	823.54	0.061083169	1324.0	1.655
0.5	1.1676E-01	823.54	0.061083169	165.5	0.207
0.75	7.7839E-02	823.54	0.061083169	49.0	0.061
1	5.8380E-02	823.54	0.061083169	20.7	0.026
1.25	4.6704E-02	823.54	0.061083169	10.6	0.013
1.5	3.8920E-02	823.54	0.061083169	6.1	0.008
1.75	3.3360E-02	823.54	0.061083169	3.9	0.005
2	2.9190E-02	823.54	0.061083169	2.6	0.003

**Table XI** Radial section for fracture aperture analysis.

Fracture aperture mm	Average Fluid Velocity m/s	Reynolds Number	Overall Reynolds	Friction Factor	Pressure Drop psia	Pressure Gradient psia/m
0.25	1.025605	3616.959068	1.05E+08	0.013908	726.158276	7.268968
0.5	0.512803	3616.959068	5.24E+07	0.013908	90.769784	0.908621
0.75	0.341868	3616.959068	3.50E+07	0.013908	26.894751	0.2692210
1	0.256401	3616.959068	2.62E+07	0.013908	11.346223	0.113578
1.25	0.205121	3616.959068	2.10E+07	0.013908	5.809266	0.058152
1.5	0.170934	3616.959068	1.75E+07	0.013908	3.361844	0.033653
1.75	0.146515	3616.959068	1.50E+07	0.013908	2.117080	0.021192
2	0.128201	3616.959068	1.31E+07	0.013908	1.418278	0.014197

**Table XII** Fracture aperture analysis results.

Injection pressure psia	Production pressure psia	Total reservoir $\Delta P$ psia	Bottom hole injection pressure psia	Pressure at injection external radius psia	Pressure at production external radius psia	Bottom hole production pressure psia
5331.2	2897.2	2776.36	11388.2	10662.0	9338.0	8611.8
4116.6	4111.9	347.05	10173.5	10082.8	9917.2	9826.5
3994.5	4234.0	102.83	10051.4	10024.5	9975.5	9948.6
3964.7	4263.7	43.38	10021.7	10010.3	9989.7	9978.3
3954.2	4274.3	22.21	10011.1	10005.3	9994.7	9988.9
3949.5	4279.0	12.85	10006.4	10003.1	9996.9	9993.6
3947.1	4281.3	8.09	10004.0	10001.9	9998.1	9996.0
3945.8	4282.7	5.42	10002.7	10001.3	9998.7	9997.3
		Distance along reservoir	0	100	900	1000

## Fracture Width

**Table XIII** Inputs for fracture width analysis.

Inputs	Symbol	Value	Units
Fracture Aperture	h	0.5	mm
Mass Flow rate	m	100	kg/s
Distance between wells	L	1000	m
Number of fractures	n	10	-
Angle for Radial Flow	$\theta$	180	$^{\circ}$
Reservoir Temperature	$T_r$	250	$^{\circ}C$
Rock Relative Roughness	$\varepsilon/h$	0.5	m
Reservoir Overburden	$P_r$	10000	psia
Injection Pressure Drop	$\Delta P_i$	-6057	psia
Production Pressure Drop	$\Delta P_p$	5715	psia

**Table XIV** Reservoir calculated data for fracture width analysis.

Reservoir Calculated Data	Symbol	Value	Units
Well radius	$r_w$	0.1016	m
Water Density	$\rho$	856.464211	kg/m <sup>3</sup>
Water Viscosity	$\mu$	1.2143E-04	kg.m.s
Fracture Aperture	h	5.0000E-04	m

**Table XV** Linear section for fracture width analysis.

Fracture Width m	Linear section length m	Fluid velocity m/s	Reynolds number	Friction factor	Pressure drop psia	Pressure gradient Psia/m
50	950	4.6704E-01	3294.16	0.015270792	786.2	0.828
75	925	3.1136E-01	2196.10	0.022906188	510.3	0.552
125	875	1.8681E-01	1317.66	0.038176981	289.6	0.331
150	850	1.5568E-01	1098.05	0.045812377	234.5	0.276
175	825	1.3344E-01	941.19	0.053447773	195.1	0.236
200	800	1.1676E-01	823.54	0.061083169	165.5	0.207
225	775	1.0379E-01	732.03	0.068718565	142.5	0.184
250	750	9.3407E-02	658.83	0.076353961	124.1	0.166

**Table XVI** Radial section for fracture width analysis.

Average Fluid Velocity m/s	External Radius m	Reynolds Number	Overall Reynolds	Friction factor	Pressure Drop psia	Pressure gradient psia/m
1.64	25	11593.02	5.24E+07	0.004339195	72.5	2.91229732
1.17	37.5	8286.59	5.24E+07	0.006070572	77.9	2.081686294
0.76	62.5	5395.76	5.24E+07	0.009322938	84.6	1.355476813
0.66	75	4622.87	5.24E+07	0.010881625	87.0	1.161317961
0.57	87.5	4054.17	5.24E+07	0.012408069	89.0	1.018452333
0.51	100	3616.96	5.24E+07	0.013907919	90.8	0.908621004
0.46	112.5	3269.65	5.24E+07	0.015385241	92.3	0.821373349
0.42	125	2986.65	5.24E+07	0.016843093	93.7	0.750279466

**Table XVII** Fracture width analysis results.

Injection pressure psia	Production pressure psia	Total reservoir ΔP psia
4408.637547	9534.412071	931.1758577
4276.056202	9666.993417	666.0131665
4172.446818	9770.6028	458.7944
4147.263783	9795.785835	408.4283301
4129.590954	9813.458665	373.0826705
4116.572326	9826.477292	347.0454154
4106.63013	9836.419488	327.1610238
4098.823016	9844.226603	311.5467945

Bottom hole injection pressure psia	Distance along reservoir m	Pressure at injection external radius psia	Distance along reservoir m	Pressure at production external radius psia	Distance along reservoir m	Bottom hole production pressure psia	Distance along reservoir m
10465.5879	0	10393.0763	25	9606.92361	975	3819.80840	1000
10333.0065	0	10255.1548	37.5	9744.84515	962.5	3952.38975	1000
10229.3972	0	10144.8176	62.5	9855.18238	937.5	4055.99913	1000
10204.2141	0	10117.2333	75	9882.76669	925	4081.18217	1000
10186.5413	0	10097.5302	87.5	9902.46976	912.5	4098.85500	1000
10173.5227	0	10082.7529	100	9917.24707	900	4111.87362	1000
10163.5805	0	10071.2594	112.5	9928.74053	887.5	4121.81582	1000
10155.7734	0	10062.0646	125	9937.93530	875	4129.62293	1000

## Number of Fractures

**Table XVIII** Inputs for number of fractures analysis.

Inputs	Symbol	Value	Units
Fracture Aperture	h	0.5	mm
Fracture Breadth	w	200	m
Distance between wells	L	1000	m
Mass Flow rate	m	100	kg/s
Angle for Radial Flow	$\theta$	180	°
Reservoir Temperature	$T_r$	250	°C
Rock Relative Roughness	$\varepsilon/h$	0.5	m
Reservoir Overburden	$P_r$	10000	psia
Injection Pressure Drop	$\Delta P_i$	-6057	psia
Production Pressure Drop	$\Delta P_p$	5715	psia

**Table XIX** Reservoir calculated data for number of fractures analysis.

Reservoir calculated data	Symbol	Value	Units
External Radius	$r_e$	100	m
Linear Section Length	$L'$	800	m
well radius	$r_w$	0.1016	m
Water Density	$\rho$	856.464211	kg/m <sup>3</sup>
Water Viscosity	$\mu$	1.2143E-04	kg.m.s
Fracture Aperture	h	5.0000E-04	m

**Table XX** Linear section for number of fractures analysis.

Number of fractures	Fluid velocity m/s	Reynolds Number	Friction Factor	Pressure Drop psia	Pressure Gradient psia/m
2.5	4.6704E-01	3294.16	0.015270792	662.0	0.828
5	2.3352E-01	1647.08	0.030541584	331.0	0.414
10	1.1676E-01	823.54	0.061083169	165.5	0.207
20	5.8380E-02	411.77	0.122166338	82.8	0.103
30	3.8920E-02	274.51	0.183249506	55.2	0.069
40	2.9190E-02	205.88	0.244332675	41.4	0.052
50	2.3352E-02	164.71	0.305415844	33.1	0.041
100	1.1676E-02	82.35	0.610831688	16.6	0.021

**Table XXI** Radial section for number of fractures analysis.

Number of fractures	Avg Fluid Velocity	Reynolds Number	Overall Reynolds	Friction Factor	Pressure Drop	Pressure Gradient
2.5	2.05	14467.84	2.10E+08	0.00347698	363.1	3.634484014
5	1.03	7233.92	1.05E+08	0.006953959	181.5	1.817242007
10	0.51	3616.96	5.24E+07	0.013907919	90.8	0.908621004
20	0.26	1808.48	2.62E+07	0.027815837	45.4	0.454310502
30	0.17	1205.65	1.75E+07	0.041723756	30.3	0.302873668
40	0.13	904.24	1.31E+07	0.055631674	22.7	0.227155251
50	0.10	723.39	1.05E+07	0.069539593	18.2	0.181724201
100	0.05	361.70	5.24E+06	0.139079186	9.1	0.0908621

**Table XXII** Number of fractures analysis results.

Injection pressure psia	Production pressure psia	Total reservoir $\Delta P$ psia	Bottom hole injection pressure psia	Pressure at injection external radius psia	Pressure at production external radius psia	Bottom hole production pressure psia
4637.140449	3591.305506	1388.181661	10694.09083	10331.01169	9668.988307	9305.909169
4290.095034	3938.350921	694.0908307	10347.04542	10165.50585	9834.494154	9652.954585
4116.572326	4111.873629	347.0454154	10173.52271	10082.75292	9917.247077	9826.477292
4029.810972	4198.634982	173.5227077	10086.76135	10041.37646	9958.623538	9913.238646
4000.890521	4227.555434	115.6818051	10057.8409	10027.58431	9972.415692	9942.159097
3986.430295	4242.015659	86.76135384	10043.38068	10020.68823	9979.311769	9956.619323
3977.75416	4250.691795	69.40908307	10034.70454	10016.55058	9983.449415	9965.295458
3960.401889	4268.044066	34.70454154	10017.35227	10008.27529	9991.724708	9982.647729
		Distance along reservoir	0	100	900	1000

## Roughness

**Table XXIII** Roughness pressure drop analysis results.

Fracture Aperture mm	Cubic law pressure drop psia	$\epsilon/h = 0.25$ pressure drop psia	$\epsilon/h = 0.25$ pressure drop psia
0.25	1324.59102	1837.87004	2776.363323
0.5	165.5738775	229.733755	347.0454154
0.75	49.05892666	68.06926074	102.8282712
1	20.69673468	28.71671937	43.38067692
1.25	10.59672816	14.70296032	22.21090658
1.5	6.132365832	8.508657592	12.8535339
1.75	3.861781399	5.358221691	8.094353711
2	2.587091835	3.589589922	5.422584615

## Reservoir Temperature

**Table XXIV** Inputs for reservoir temperature analysis.

Inputs	Symbol	Value	Units
Fracture Aperture	h	0.5	mm
Fracture Breadth	w	200	m
Distance between wells	L	1000	m
Number of fractures	n	10	-
Angle for Radial Flow	$\theta$	180	$^\circ$
Mass Flow Rate	m	100	kg/s
Rock Relative Roughness	$\epsilon/h$	0.5	m
Reservoir Overburden	$P_r$	10000	psia
Injection Pressure Drop	$\Delta P_i$	-6057	psia
Production Pressure Drop	$\Delta P_p$	5715	psia

**Table XXV** Reservoir calculated data for reservoir temperature analysis.

Reservoir Calculated Data	Symbol	Value	Units
External Radius	$r_e$	100	m
Linear Section Length	$L'$	800	m
well radius	$r_w$	0.1016	m
Fracture Aperture	$h$	5.0000E-04	m

**Table XXVI** Linear section for reservoir temperature analysis.

Reservoir Temperature °C	Water Density $kg/m^3$	Water Viscosity Pa.s	Fluid Velocity m/s	Reynolds Number	Friction Factor	Pressure Drop psia	Pressure Gradient psia/m
125	970.6293714	0.000239524	1.0303E-01	417.49	0.120491243	288.1	0.360
150	951.4640069	0.00019897	1.0510E-01	502.59	0.100090835	244.1	0.305
175	930.491626	0.000170489	1.0747E-01	586.55	0.085763188	213.9	0.267
200	907.7186137	0.000149651	1.1017E-01	668.22	0.075280902	192.5	0.241
225	883.085246	0.000133841	1.1324E-01	747.16	0.067327702	176.9	0.221
250	856.464211	0.000121427	1.1676E-01	823.54	0.061083169	165.5	0.207
275	827.6518725	0.000111342	1.2082E-01	898.14	0.056009757	157.0	0.196
300	796.3529116	0.000102849	1.2557E-01	972.30	0.051737606	150.8	0.188

**Table XXVII** Radial section for reservoir temperature analysis.

Res Temp °C	Water Density $kg/m^3$	Water Viscosity Pa.s	Average fluid velocity m/s	Reynolds Number	Overall Reynolds	Friction Factor	Pressure Drop psia	Pressure Gradient psia/m
125	970.6293	0.00023952	0.45	1833.6	2.66E+07	0.02743	158.0	1.5815119
150	951.4640	0.00019897	0.46	2207.3	3.20E+07	0.02278	133.9	1.3402085
175	930.4916	0.00017048	0.47	2576.1	3.73E+07	0.01952	117.3	1.1742454
200	907.7186	0.00014965	0.48	2934.8	4.25E+07	0.01714	105.6	1.0565839
225	883.0852	0.00013384	0.50	3281.4	4.76E+07	0.01539	97.0	0.9713183
250	856.4642	0.00012142	0.51	3616.9	5.24E+07	0.01390	90.8	0.9086210
275	827.6517	0.00011134	0.53	3944.5	5.72E+07	0.01275	86.1	0.8621571
300	796.3529	0.00010284	0.55	4270.3	6.19E+07	0.01178	82.7	0.8276966

**Table XXVIII** Reservoir temperature analysis results for production well.

Production Density $kg/m^3$	Production Viscosity Pa.s	Velocity m/s	Reynolds	f	Production $\Delta P$ psia
967.6069693	0.000254519	3.186865419	2461877.551	0.014450938	6423.355307
948.7621207	0.000207773	3.250164738	3015758.998	0.014383287	6306.138676
927.8653787	0.000175603	3.323362699	3568234.783	0.014335933	6176.7778
904.9444665	0.000152452	3.407538588	4110121.144	0.014301436	6035.416227
879.9321116	0.000135119	3.504398975	4637349.277	0.014275376	5881.677645
852.6684582	0.000121655	3.616450404	5150600.191	0.01425499	5714.67329
822.8904972	0.000110802	3.747318994	5655073.137	0.014238467	5532.946153
790.2081246	0.000101709	3.902305094	6160654.499	0.014224559	5334.350695

**Table XXIX** Reservoir temperature analysis results.

<b>Injection pressure psia</b>	<b>Total reservoir <math>\Delta P</math> psia</b>	<b>Bottom hole injection pressure psia</b>	<b>Pressure at injection external radius psia</b>	<b>Pressure at production external radius psia</b>	<b>Bottom hole production pressure psia</b>
4245.076802	604.0543678	10302.02718	10144.03667	9855.963334	9697.972816
4198.994191	511.8891448	10255.94457	10122.05988	9877.940116	9744.055428
4167.299605	448.4999739	10224.24999	10106.94475	9893.055254	9775.750013
4144.829355	403.5594737	10201.77974	10096.22869	9903.771309	9798.220263
4128.545872	370.9925062	10185.49625	10088.4631	9911.536897	9814.503747
4116.572326	347.0454154	10173.52271	10082.75292	9917.247077	9826.477292
4107.698945	329.2986539	10164.64933	10078.52121	9921.478789	9835.350673
4101.117902	316.1365668	10158.06828	10075.38271	9924.617287	9841.931717
	<b>Distance along reservoir m</b>	<b>0</b>	<b>100</b>	<b>900</b>	<b>1000</b>